Neuron
Article

A Combinatorial Semaphorin Code Instructs the Initial Steps of Sensory Circuit Assembly in the *Drosophila* CNS

Zhuhao Wu,[1] Lora B. Sweeney,[2] Joseph C. Ayoob,[1,4] Kayam Chak,[1] Benjamin J. Andreone,[1] Tomoko Ohyama,[3] Rex Kerr,[3] Liqun Luo,[2] Marta Zlatic,[3] and Alex L. Kolodkin[1,*]
[1]The Solomon H. Snyder Department of Neuroscience, The Johns Hopkins University School of Medicine, Howard Hughes Medical Institute, Baltimore, MD 21205, USA
[2]Department of Biology and Neurosciences Program, Howard Hughes Medical Institute, Stanford University, Stanford, CA 94305, USA
[3]Janelia Farm Research Campus, Howard Hughes Medical Institute, Ashburn, VA 20147, USA
[4]Present address: Department of Computational and Systems Biology, University of Pittsburgh School of Medicine, Pittsburgh, PA 15207, USA
*Correspondence: kolodkin@jhmi.edu
DOI 10.1016/j.neuron.2011.02.050

SUMMARY

Longitudinal axon fascicles within the *Drosophila* embryonic CNS provide connections between body segments and are required for coordinated neural signaling along the anterior-posterior axis. We show here that establishment of select CNS longitudinal tracts and formation of precise mechanosensory afferent innervation to the same CNS region are coordinately regulated by the secreted semaphorins Sema-2a and Sema-2b. Both Sema-2a and Sema-2b utilize the same neuronal receptor, plexin B (PlexB), but serve distinct guidance functions. Localized Sema-2b attraction promotes the initial assembly of a subset of CNS longitudinal projections and subsequent targeting of chordotonal sensory afferent axons to these same longitudinal connectives, whereas broader Sema-2a repulsion serves to prevent aberrant innervation. In the absence of Sema-2b or PlexB, chordotonal afferent connectivity within the CNS is severely disrupted, resulting in specific larval behavioral deficits. These results reveal that distinct semaphorin-mediated guidance functions converge at PlexB and are critical for functional neural circuit assembly.

INTRODUCTION

Neurons extend processes over long distances during development, establishing complex yet precise connections to achieve mature neuronal functions. During this process growing neuronal processes recognize and interpret numerous cues as they navigate to their appropriate targets (Raper and Mason, 2010; Tessier-Lavigne and Goodman, 1996). In both vertebrates and invertebrates, longitudinal neural tracts extending along the anterior-posterior axis within the nerve cord serve to exchange and integrate information between different body segments and the brain. To establish these tracts, developing neurites must extend across segmental boundaries, often fasciculating with related neurites from a myriad of possible partners in adjacent segments. In addition, longitudinal pathways often receive neural input from sensory afferents and other local interneurons critical for processing specific sensory information and modulating appropriate motor responses. These two aspects of longitudinal tract assembly could be intrinsically linked to better achieve select targeting of neuronal projections that belong to the same circuit.

Cellular experiments in both invertebrates and vertebrates demonstrate the importance of contact with pioneer neurons for the establishment of continuous rostral-caudal neuronal pathways (Goodman et al., 1984; Kuwada, 1986; Wolman et al., 2008). Genetic analyses in the *Drosophila* embryonic CNS reveal molecular mechanisms governing important aspects of longitudinal pathway organization within the nerve cord. The initial projections of some CNS axons that extend longitudinally are first guided by selectively localized netrin on the surface of adjacent axons (Hiramoto et al., 2000). Subsequently, these axons lose their responsiveness to netrin, continue projecting longitudinally, and cross segmental boundaries through the action of Slit/Robo signaling (Hiramoto and Hiromi, 2006). Slit-mediated repulsion specifies three lateral positions (medial, intermediate, and lateral) for distinct longitudinal axon tracts based on differential expression of Robo receptors (Evans and Bashaw, 2010; Rajagopalan et al., 2000; Simpson et al., 2000; Spitzweck et al., 2010). Related functions of Slit-Robo signaling for CNS longitudinal tract formation have also been observed in vertebrates (Farmer et al., 2008; Long et al., 2004; Lopez-Bendito et al., 2007; Mastick et al., 2010). Interestingly, sensory afferent input to the *Drosophila* embryonic CNS utilizes this same Slit-Robo code to regulate the projection of different sensory axon classes to distinct CNS lateral positions (Zlatic et al., 2003), restricting both the pre- and postsynaptic components of this first synapse for sensory circuits to a limited region. It remains to be determined how neuronal projections within these specific regions selectively fasciculate with one another.

Several homophilic cell adhesion molecules, including FasII, L1, and Tag1, have been observed to promote the fasciculation of CNS longitudinal projections (Harrelson and Goodman, 1988; Lin et al., 1994; Wolman et al., 2007; Wolman et al., 2008). In the grasshopper and in *Drosophila*, anti-FasII monoclonal antibodies (MAbs) specifically label several longitudinal fascicles on each side of the CNS, and in *Drosophila* (utilizing the 1D4 mAb) these appear as three discrete longitudinal axon tracts when viewed from a dorsal aspect (Bastiani et al., 1987; Grenningloh et al., 1991; Landgraf et al., 2003). However, the 1D4-positive ($1D4^+$) tracts in the *Drosophila* embryonic CNS represent only a small subset of the total CNS longitudinal pathways within each lateral region specified by the Slit-Robo code, and they are closely associated with other longitudinal projections that are 1D4-negative (Bastiani et al., 1987; Lin et al., 1994; Rajagopalan et al., 2000; Simpson et al., 2000). Chordotonal (ch) sensory afferent inputs to the CNS, which specifically exhibit axonal branching and elongation along the intermediate $1D4^+$ longitudinal tract (Zlatic et al., 2003), are also 1D4-negative. Taken together, these observations suggest that additional factors govern these specific fasciculation events within each CNS region.

Repulsive semaphorin guidance cues signaling through their cognate plexin receptors have been implicated in longitudinal tract formation and in the restriction of sensory afferent projections to distinct CNS targets in both *Drosophila* and mouse (Pecho-Vrieseling et al., 2009; Yoshida et al., 2006; Zlatic et al., 2009). In *Drosophila*, Plexin A (PlexA) and Plexin B (PlexB) are the only plexin receptors, and both play important roles during CNS longitudinal tract development. PlexA is the receptor for transmembrane semaphorin-1a (Sema-1a) and is required for CNS longitudinal tract formation, however only in the most lateral region of the nerve cord (Winberg et al., 1998b). The PlexB receptor, in contrast, is specifically required for the organization of CNS longitudinal tract only in the intermediate region (Ayoob et al., 2006), however the identity of the PlexB ligand(s) required for this function is still unclear. There are two secreted semaphorins in *Drosophila*, semaphorin-2a (Sema-2a) and semaphorin-2b (Sema-2b). Sema-2a signals repulsion and contributes in part to PlexB-mediated sensory afferent targeting within the CNS; however, CNS longitudinal projections appear to be less affected in *Sema-2a* mutants as compared to *PlexB* mutants (Zlatic et al., 2009).

Here, we show that both Sema-2a and Sema-2b are PlexB ligands during embryonic CNS development and mediate distinct functions. The PlexB receptor integrates both Sema-2a repulsion and Sema-2b attraction to coordinately regulate the assembly of specific CNS longitudinal projections and select sensory afferent innervation within that same CNS region. Perturbation of PlexB-mediated signaling during the establishment of sensory afferent connectivity within the CNS results in larval sensory-dependent behavioral deficits. These results suggest that a combination of semaphorin cues, acting in concert with the longer-range Slit gradient in the embryonic *Drosophila* CNS, ensures the fidelity of both CNS interneuron projection organization and sensory afferent targeting, both of which are critical for the establishment of a functional neural circuit.

RESULTS

PlexB Is Required for Appropriate Projection of Both CNS Interneurons and ch Sensory Afferents within the Intermediate Domain of the Embryonic *Drosophila* CNS

In the absence of *PlexB*, interneuron projections that form a group of longitudinal connectives in the developing *Drosophila* embryonic CNS are disorganized (Ayoob et al., 2006). Interestingly, the targeting of ch sensory afferent projections to the CNS occurs within this same intermediate CNS region, as determined by intracellular labeling of individual ch neurons (Merritt and Whitington, 1995; Zlatic et al., 2003). By genetically labeling ch neurons with GFP using the *iav-GAL4* driver (Kwon et al., 2010) and visualizing CNS longitudinal tracts with 1D4 immunohistochemistry (Figures 1A–1D), we asked whether or not sensory afferent targeting to the CNS also requires PlexB. As previously reported (Ayoob et al., 2006), in $PlexB^{-/-}$ null mutant ($PlexB^{KG00878}$) embryos the intermediate $1D4^+$ longitudinal tract (1D4-i) is severely disorganized (including defasciculation, disorganization, and wandering of axon bundles within this intermediate position); however, the medial and lateral $1D4^+$ tracts (1D4-m and 1D4-l) appear normal (Figures 1E and 1F). In $PlexB^{-/-}$ mutants, ch axons extend into the CNS but fail to form regular terminal branches in the region of the disrupted 1D4-m tract, instead remaining stalled with expanded, splayed out, morphologies over the region where they normally would elaborate their synaptic contacts (Figures 1G and 1H). The other plexin receptor in *Drosophila*, PlexA, is required for the formation of the 1D4-l tract but not the 1D4-i tract, and in $PlexA^{-/-}$ mutants ch afferent projections target to the medial region of the CNS in a relatively normal fashion (see Figures S1A–S1D available online). These results show that PlexB-mediated signaling is required for appropriate projection of both CNS interneurons and ch sensory afferents to the same intermediate region within the developing CNS.

Both Sema-2a and Sema-2b Are PlexB Ligands Required for Appropriate Projection of CNS Interneurons within the Intermediate Longitudinal Region

During *Drosophila* embryonic neural development, the 1D4-i tract is established before ch sensory afferent targeting and elongation along this tract (Figures S1E–S1J). Therefore, we first addressed how PlexB regulates the formation of the 1D4-i tract within the CNS by defining the ligands required for this function. The semaphorin protein Sema-2a is thought to be a PlexB ligand in both the PNS and CNS (Ayoob et al., 2006; Bates and Whitington, 2007; Zlatic et al., 2009). However, previous analyses using different P element-derived $Sema\text{-}2a^{-/-}$ mutant alleles show no, or very weak, CNS $1D4^+$ longitudinal tract phenotypes (Winberg et al., 1998a; Zlatic et al., 2009). To address the involvement of Sema-2a in CNS development, we made a *Sema-2a* null allele by generating an FRT-derived genomic deletion called $Sema\text{-}2a^{B65}$ (see Figure S2A for details). $Sema\text{-}2a^{B65}$ null mutant embryos do show pronounced CNS 1D4-i tract defasciculation defects (Figure 2C); however, the phenotypes are less severe than those observed in $PlexB^{-/-}$ mutants (Figures 2B and 2I). Therefore, there must be at least one additional PlexB ligand that functions to organize CNS longitudinal projections.

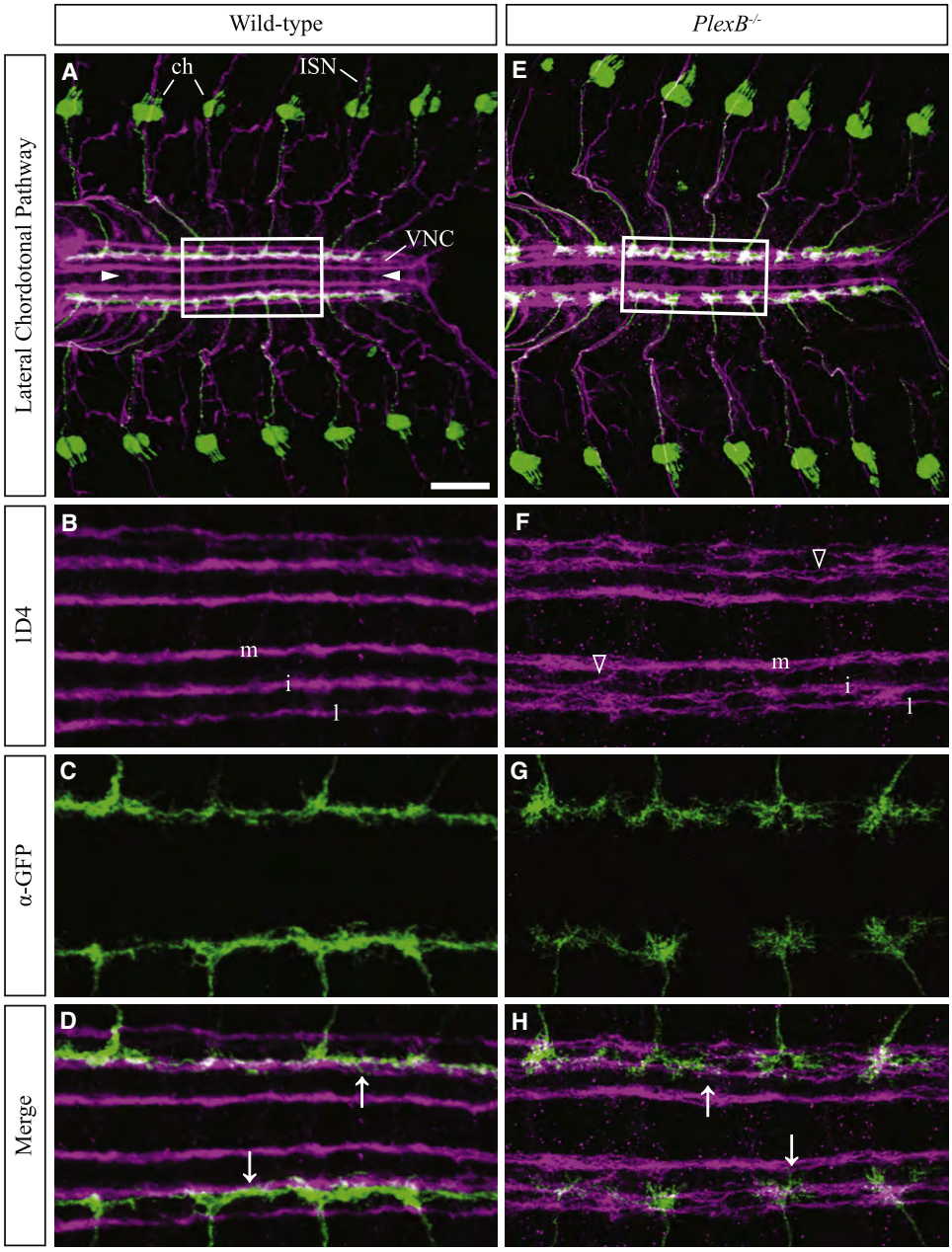

Figure 1. PlexB Is Required for the Organization of Select CNS Longitudinal Connectives and Chordotonal Sensory Afferent Innervation within the Embryonic *Drosophila* CNS

(A–D) In wild-type late stage 16 *Drosophila* embryos lateral chordotonal (ch) neurons extend axons toward the ventral nerve cord (VNC) along the intersegmental nerve (ISN) pathway. Embryos were stained with 1D4 (magenta) and anti-GFP (green), and then filleted from the dorsal side to generate a flat-mount preparation (anterior is to the left, arrowheads mark the CNS ventral midline). 1D4 staining reveals all peripheral motor axon projections and three longitudinally projecting CNS axon tracts (l, lateral; i, intermediate; m, medial) on both sides of the VNC. The *iav-GAL4* driver directs *UAS:syt-GFP* expression in ch sensory neurons, which preferentially label terminal branches in their afferent innervations to the CNS. The CNS regions boxed in (A) are shown at higher magnification in (B–D). Wild-type ch sensory axons target their terminal branches to a region close to the 1D4-i tract. Scale bar represents 30 μm for (A); 10 μm for (B)–(D).

(E–H) In *PlexB*$^{-/-}$ mutant embryos, ch axons project normally in the periphery along the ISN pathway to the CNS. However, within the CNS the 1D4-i tract is disorganized (empty arrowheads in F), and ch axons fail to elaborate their characteristic regular and continuous CNS innervation pattern (arrows in H). The CNS regions boxed in (E) are shown at higher magnification in (F–H). Scale bar represents 30 μm for (E); 10 μm for (F)–(H). See also Figure S1.

Of the four other *Drosophila* semaphorins, the secreted semaphorin Sema-2b is the best candidate PlexB ligand. Sema-5c is not expressed in the CNS during the embryonic development (Khare et al., 2000), and Sema-1a and Sema-1b bind to PlexA but not to PlexB (Ayoob et al., 2006; Winberg et al., 1998b). The Sema-2b protein is most closely related to Sema-2a,

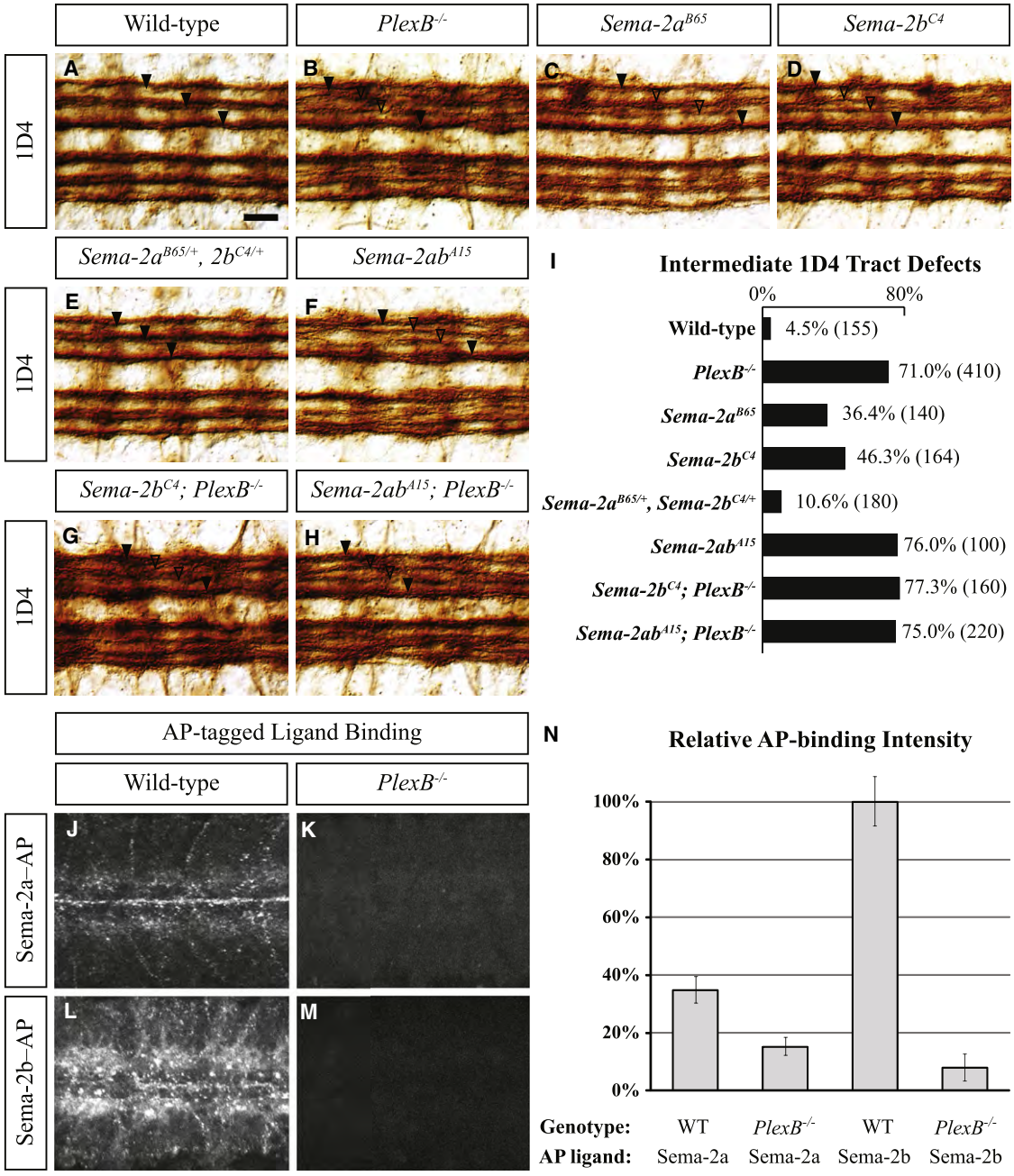

Figure 2. Secreted Semaphorins Sema-2a and Sema-2b Are Both PlexB Ligands and Are Required for Select CNS Longitudinal Tract Formation

(A–H) Dorsal views of the late stage 16 embryonic CNS in different genetic backgrounds, all labeled with the 1D4 mAb. Solid arrowheads indicate regular, continuous 1D4$^+$ CNS longitudinal tracts; empty arrowheads indicate disorganized and defasciculated 1D4$^+$ tracts. Scale bar represents 10 μm (A–H).

(I) Quantification of the 1D4-i defects. Percentages of disorganized hemisegments are shown, with the total number (n) of hemisegments scored in parentheses (see Experimental Procedures for detailed scoring methods).

(J–M) Alkaline phosphatase (AP)-tagged ligands were applied to wild-type and *PlexB*$^{-/-}$ live-dissected embryonic ventral nerve cords (VNCs). Scale bar represents 12 μm (J–M).

(N) Comparison of AP-ligand embryonic VNC binding intensities (all normalized to Sema-2b-AP binding to wild-type VNC). Error bars indicate standard deviation. See also Figure S2.

exhibiting 68% amino acid sequence identity. To analyze Sema-2b function, we made a *Sema-2b* null mutant by generating an FRT-derived genomic deletion called *Sema-2b*^{C4} (see Figure S2A for details). *Sema-2b*^{C4} null mutant embryos show pronounced disorganization and defasciculation defects in the 1D4-i tract (Figure 2D), suggesting that Sema-2b also serves as a PlexB

ligand during the embryonic CNS development. However, the CNS phenotypes observed in *Sema-2b*^{C4} null mutants are also not as severe as those observed in the *PlexB*$^{-/-}$ mutant (Figures 2B and 2I). To ask whether both Sema-2a and Sema-2b are required for PlexB-mediated functions, we generated a *Sema-2a*, *Sema-2b* double null allele called *Sema-2ab*^{A15} (see Figure S2A for details). *Sema-2ab*^{A15} homozygous mutant embryos fully recapitulate the phenotypes observed in *PlexB*$^{-/-}$ mutants regarding defects in the 1D4-i tract (Figures 2F and 2I). We also analyzed *Sema-2b*^{C4}*;PlexB* double null mutant embryos (Figure 2G) and *Sema-2ab*^{A15}*;PlexB* double null mutant embryos (that are null for *Sema2a*, *Sema2b*, and *PlexB*) (Figure 2H); both genotypes exhibit 1D4-i defects identical to those observed in *PlexB*$^{-/-}$ single mutants and *Sema-2ab*^{A15} homozygous mutants with equal penetrance (Figure 2I), indicating that both *Sema-2a* and *Sema-2b* function in the same genetic pathway as *PlexB*. Interestingly, *Sema-2a*^{B65}/+, *Sema-2b*^{C4}/+ *trans*-heterozygous mutant embryos exhibit a much lower penetrance of CNS longitudinal connective defects than embryos of either single mutant (Figures 2E and 2I), suggesting that Sema-2a and Sema-2b functions are distinct and contribute to different aspects of intermediate longitudinal connection formation.

To complement our genetic analyses we next performed alkaline phosphatase (AP)-tagged ligand binding assays on live dissected embryos (Fox and Zinn, 2005). We first confirmed that AP alone does not bind to the CNS of dissected *Drosophila* embryos in our assay (data not shown). We then observed that Sema-2a-AP and Sema-2b-AP both bound to endogenous CNS receptors in dissected wild-type embryos (Figures 2J and 2L), but not to endogenous CNS receptors in *PlexB*$^{-/-}$ mutants (Figures 2K and 2M). Compared to Sema-2a-AP, Sema-2b-AP bound more robustly to endogenous CNS receptors (Figure 2N). We also expressed PlexB in a *Drosophila* S2R+ cell line and observed that Sema-2b-AP bound strongly to these cells but not to PlexA-expressing S2R+ cells (Figures S2G and S2D), as observed previously for Sema-2a (Ayoob et al., 2006) (Figures S2B–S2F). These ligand-receptor binding specificities correlate well with the functions of these proteins in CNS longitudinal track formation. *PlexB*$^{-/-}$ and *PlexA*$^{-/-}$ mutant embryos exhibit distinct CNS longitudinal tract defects (Ayoob et al., 2006; Winberg et al., 1998b), and *Sema-1a*$^{-/-}$ mutants have defects similar to those observed in *PlexA*$^{-/-}$, but not *PlexB*$^{-/-}$, mutants (Yu et al., 1998) (Figures S2H and S2I). In addition, we observed that *Sema-1a*, *Sema-2b* double null mutants and *Sema-1a;PlexB* double null mutants both show disorganization of the 1D4-l and 1D4-m tracts (Figures S2J and S2K), further supporting the idea that *Sema-1a-PlexA* and *Sema-2b-PlexB* signaling direct distinct aspects of embryonic longitudinal tract formation. Taken together, these results show that Sema-2a and Sema-2b signaling through the PlexB receptor accounts for most, if not all, PlexB functions in embryonic CNS intermediate longitudinal tract formation.

Sema-2b Protein Is Expressed along Specific CNS Longitudinal Connectives and Functions to Promote Select Longitudinal Connective Assembly

We next assessed Sema-2b protein distribution in *Drosophila* embryos using a polyclonal antibody specific for Sema-2b (L.B.S., Y. Chou, Z.W., T. Komiyama, C.J. Potter, A.L.K., K.C. Garcia, and L.L., unpublished data). Sema-2b is weakly expressed on CNS commissures and more robustly on two longitudinal pathways (Figure 3B). Sema-2b expression is strong along the 1D4-i tract, and also is localized on a more medial pathway that lies directly adjacent to the 1D4-m tract (Figure 3C). Sema-2b protein is completely absent in *Sema-2b*^{C4} null mutant embryos (Figure 3D).

To better define Sema-2b CNS expression, we labeled Sema-2b-expressing neurons and their processes using a genomic fragment containing ~35 kb of DNA upstream of the Sema-2b protein coding region to construct a Sema-2b reporter (*2b*^{L}*-τGFP*; Figure 3A). The *2b*^{L}*-τGFP* reporter labels two distinct longitudinal axon tracts, recapitulating the staining pattern for endogenous Sema-2b expression, and the outer of these two GFP^{+} tracts occupies the same lateral position as the 1D4-i connectives (Figures 3E and 3F). Sema-2b, a secreted protein, is most likely released from these *2b*^{L}*-τGFP* pathways. Therefore, the correct formation of these *2b*^{L}*-τGFP* longitudinal pathways is likely to be required for normal Sema-2b expression and, perhaps, subsequent fasciculation and organization of the 1D4-i axons. To determine if these Sema-2b-expressing pathways themselves require Sema-2b for their assembly, we first examined the *2b*^{L}*-τGFP* pathways in the *Sema-2b*^{C4} null mutant. We found that the outer *2b*^{L}*-τGFP* pathway appeared disorganized in the absence of Sema-2b, whereas the medial *2b*^{L}*-τGFP* pathway appeared to remain largely intact (Figure 3G), suggesting that Sema-2b functions in a cell-type autonomous manner to promote the fasciculation of Sema-2b-expressing longitudinal axons in the intermediate region. However, given the difficulty in discerning the integrity of these Sema-2b-expressing *2b*^{L}*-τGFP* pathways, we used the more selective *Sema2b-τMyc* (*2b-τMyc*) reporter. This reporter labels only a subset of the Sema-2b-expressing neurons in the CNS (Rajagopalan et al., 2000), and we observed that these neurons normally express very high levels of Sema-2b (Figures S3A–S3C). In wild-type embryos, neurons labeled by the *2b-τMyc* reporter line extend their axons across the midline along the anterior commissure and then turn anteriorly, subsequently fasciculating with *2b-τMyc* axons in the next anterior segment and thereby forming a continuous longitudinal connective (Figure 3H). During neural development, the *2b-τMyc*–labeled longitudinal tract is formed before the 1D4-i fascicle, which subsequently forms directly adjacent to it (Figure 3I and Figures S3D–S3L). In *Sema-2b*^{C4} null mutants, the number and cell body position of *2b-τMyc* neurons remains unchanged and their axons project normally across the CNS midline, turning anteriorly in their normal lateral position. However, they then often wander off their correct path and fail to fasciculate with *2b-τMyc* axons in the next anterior segment, resulting in an aberrant *2b-τMyc* longitudinal axon tract (Figure 3J). Some *Sema-2b*^{C4} mutant axons (~0.73 per embryo) exhibit shifting of their anterior projections to a more medial position (medial detour), however a greater fraction of misdirected *Sema-2b*^{C4} axons (~2.54 per embryo) shift laterally (lateral detour). Some *2b-τMyc* axons (~0.61 per embryo) turn and exit laterally from the anterior pathway in *Sema-2b*^{C4} mutant (lateral exit) (Figure 3J; see quantification below). These phenotypes are never observed in wild-type embryos. These results

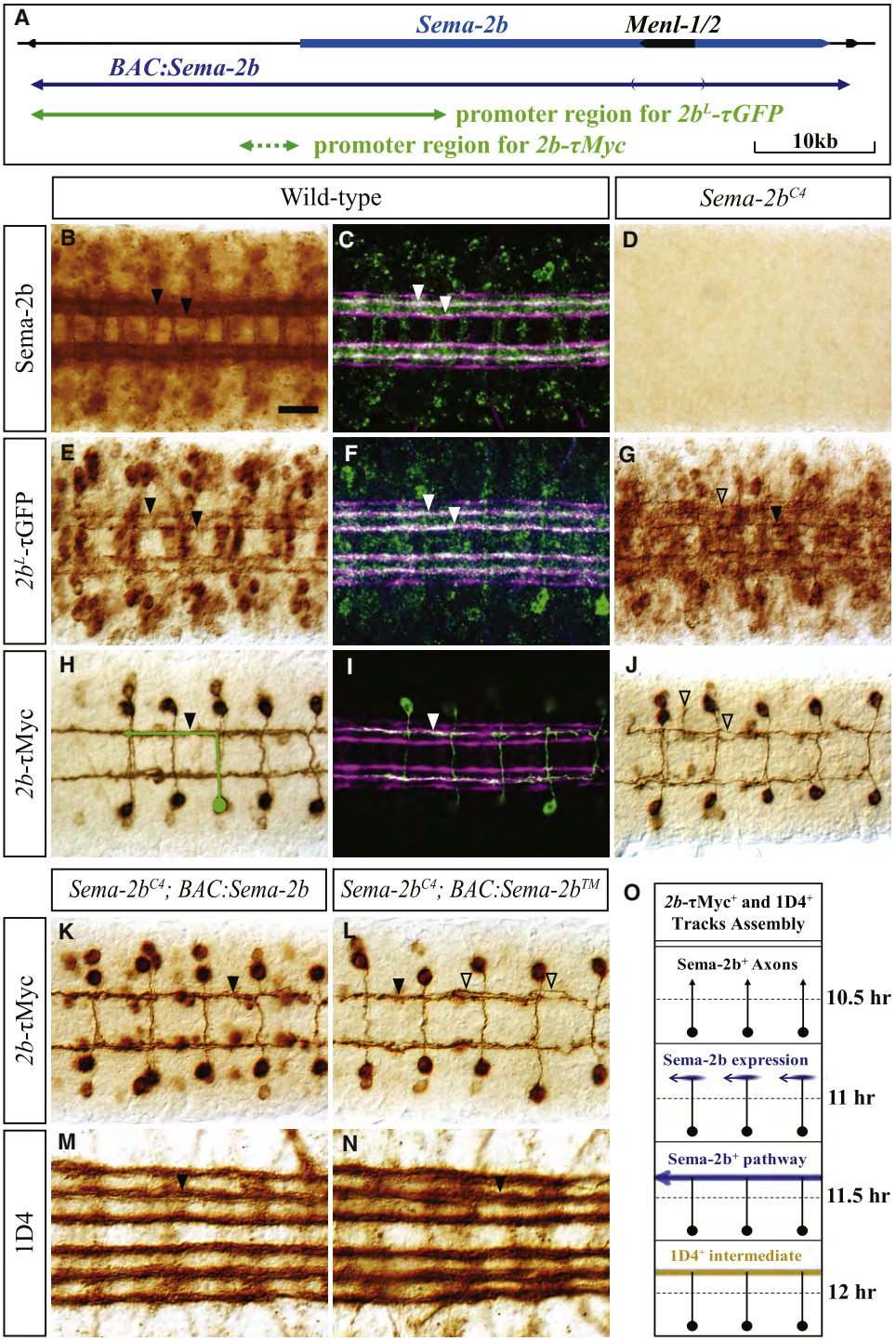

Figure 3. Sema-2b Protein Is Expressed Along Specific CNS Longitudinal Connectives and Functions to Promote the Assembly of Select Longitudinal Connectives

(A) The *Sema-2b* locus. The blue line represents the genomic region used to construct *Sema-2b* BAC transgenes (DNA containing the *Menl-1/2* genes was removed; also see Figure S2A). The solid green line covers the promoter region used to construct the Sema-2b reporter, $2b^{L}$-*τGFP*; the dashed green line represents the *Sema-2b* promoter fragment used to make the *2b-τMyc* (*Sema2b-τMyc*) reporter (Rajagopalan et al., 2000).

(B–J) CNS in stage 15/16 embryos of wild-type (B, C, E, F, H, and I) or *Sema-2b*^{C4} null mutants (D, G, and J). (B–D) Sema-2b IHC using a rabbit polyclonal antibody. (E–G) The $2b^{L}$-*τGFP* reporter labels Sema-2b-expressing neurons and their axonal trajectories. (H–J) The *2b-τMyc* reporter labels a subset of Sema-2b-expressing neurons. The axonal projection of one representative *2b-τMyc* neuron is schematically depicted in green (H). (C, F, and I) 1D4^{+} tracts are

suggest that that Sema-2b is required cell-type autonomously for *2b-τMyc* longitudinal pathway formation. Importantly, the formation of *2b-τMyc* pathway does not depend on Sema-1a or PlexA (Figures S3M and S3N).

We next restored Sema-2b expression in the *Sema-2b^{C4}* null mutant using a BAC transgene that covers only the *Sema-2b* genomic region (however, with the *Menl-1/2* genes removed; see Figure S2 for details). This ~60 kb BAC transgene (*BAC:Sema-2b*) fully rescues the *Sema-2b^{C4}* longitudinal connective defects, including those in both the *2b-τMyc^{+}* pathway and the 1D4-i tract (Figures 3K and 3M; see quantification below). To assess how secreted Sema-2b promotes the fasciculation and organization of Sema-2b-expressing longitudinal axons and also the 1D4-i tract, we conducted a similar rescue experiment using a modified BAC transgene (*BAC:Sema-2b™*) that expresses a membrane-tethered Sema-2b otherwise identical to *BAC:Sema-2b*. The *BAC:Sema-2b™* transgene also rescues most of the *Sema-2b^{C4}* null mutant phenotypes seen in both the *2b-τMyc^{+}* and the 1D4-i tracts (Figures 3L and 3N; see quantification below). We find that a small fraction (~1 axon per embryo) of the *2b-τMyc* axons are still diverted laterally in this *BAC:Sema-2b™* rescue, however unlike in the *Sema-2b^{C4}* null mutant, these pathways often rejoin *2b-τMyc* axons in the next anterior segment (Figure 3L, empty arrowhead). Therefore, expression of secreted Sema-2b serves to facilitate *2b-τMyc* axon fasciculation, and because a transmembrane Sema-2b also can function in this capacity, these results strongly suggest that Sema-2b functions at short-range as an axonally delivered guidance cue, mediating axon-axon recognition and fasciculation during *Drosophila* embryonic CNS development.

Sema-2a Is Broadly Distributed in the Embryonic CNS and Unlike Sema2b Functions as a Repellent to Position Longitudinal Tracts

Using mAb 19C2, which specifically recognizes Sema-2a (Bates and Whitington, 2007), we found that Sema-2a is concentrated along ventral midline structures and commissures during neural development, exhibits lower expression levels toward the lateral regions of the CNS and is diffusely distributed along the region of the CNS longitudinal tracts (Figure 4A). 19C2 staining is absent in *Sema-2a^{B65}* null mutant embryos (Figure 4B). The *2b-τMyc* axons cross the CNS midline along the anterior boundary of the anterior commissure and then form their longitudinal connective in a lateral CNS region where relatively lower levels of Sema-2a are found (Figure 4C). In *Sema-2a^{B65}* null mutant embryos, the *2b-τMyc^{+}* axons still remain tightly fasciculated with one another and form their characteristic continuous longitudinal pathway. However, some *2b-τMyc* axons (~0.67 per embryo) detour medially, sometimes extending to the CNS midline and crossing over to the contralateral side (~0.3 per embryo): phenotypes never observed in wild-type embryos (Figure 4D; see quantification below). These inappropriate projections are located in regions where Sema-2a is normally highly expressed in wild-type embryos. We restored Sema-2a expression in the *Sema-2a^{B65}* null mutant using a ~36Kb BAC transgene covering the entire *Sema-2a* genomic region (*BAC:Sema-2a*), resulting in full rescue of all CNS defects observed in both the *2b-τMyc* pathway and 1D4^{+} tracts (Figures 4E and 4F). Consistent with previous studies (Zlatic et al., 2009), our results suggest that Sema-2a serves as a repulsive cue to constrain axons within select regions of the CNS.

Sema-2a and Sema-2b proteins share 68% amino-acid identity, however our results suggest that they mediate distinct functions. To directly assess differences in how these closely related ligands guide axons, we performed two gain-of-function (GOF) experiments. We first asked whether Sema-2a and Sema-2b mediate distinct functions in CNS longitudinal tract formation. We engineered two different BAC constructs using the same portion of the *Sema-2b* promoter (Figure 3A), and we expressed either Sema-2a (*BAC:2b^{L}-Sema-2a*) or Sema-2b (*BAC:2b^{L}-Sema-2b*) in the *Sema-2b^{C4}* genetic background. The *BAC:2b^{L}-Sema2b* transgene fully rescued the *Sema-2b^{C4}* mutant phenotypes, (Figures 4G and 4H). In contrast, the *BAC:2b^{L}-Sema2a* transgene failed to rescue the guidance defects observed in the *Sema-2b^{C4}* mutants. Interestingly, the *BAC:2b^{L}-Sema2a* transgene did result in the appearance of more severe defects in *2b-τMyc* pathway. These mostly include individual defasciculated *2b-τMyc^{+}* axons that project laterally toward the margins of the CNS (Figure 4I; see quantification below). The 1D4-i tract was also severely disrupted and multiple ectopic crossings of the midline by 1D4^{+} axons were observed in ~90% of the segments after Sema-2a expression in the Sema-2b expressing neurons (Figure 4J; 45 of 50 segments scored), a phenotype never observed in *Sema-2b^{C4}* mutants or the corresponding *BAC:2b^{L}-Sema2b* rescue experiments. These results show that Sema-2a and Sema-2b can mediate distinct guidance functions in the same neuronal pathways.

We next asked whether or not Sema-2a and Sema-2b can also mediate distinct guidance functions in other parts of the nervous system. *Drosophila* embryonic motor pathways labeled by 1D4 show stereotypic projection patterns and innervate distinct peripheral muscles (Figures S4A, S4B, and S4E) (Bate and Broadie, 1995), providing a simple yet robust system to study guidance cue functions (Vactor et al., 1993). Using the *5053A-GAL4* line (Ritzenthaler et al., 2000), transmembrane versions of Sema-2a or Sema-2b were ectopically expressed solely on peripheral muscle-12 in developing embryos (Figure S4C). *Sema-2a™* GOF in muscle-12 led to a loss of normal ISNb RP5 innervation in ~50% of hemisegments examined (Figure 4K, empty arrowheads, and Figures S4D and S4E), consistent with the known repulsive effects of Sema-2a on embryonic motor neurons (Ayoob et al., 2006; Carrillo et al., 2010; Matthes et al., 1995; Winberg et al., 1998a), whereas Sema-2b™ GOF in muscle-12 had no affect on ISNb RP5 formation (Figure 4L, arrowheads and Figure S4D). However, Sema-2b™ overexpression in peripheral muscle-12 did have a pronounced effect on the

also labeled with anti-Sema-2b. Solid arrowheads indicate regular projection patterns; empty arrowheads indicate disorganized tracts. Scale bar represents 16 μm (B–L).

(K–N) *Sema-2b* BAC transgenes rescue the longitudinal pathway defects observed in *Sema-2b^{C4}* mutants. Scale bar represents 10 μm (M, N).

(O) Schematic depiction of Sema-2b-mediated *2b-τMyc* pathway and 1D4-i tract assembly. See also Figure S3.

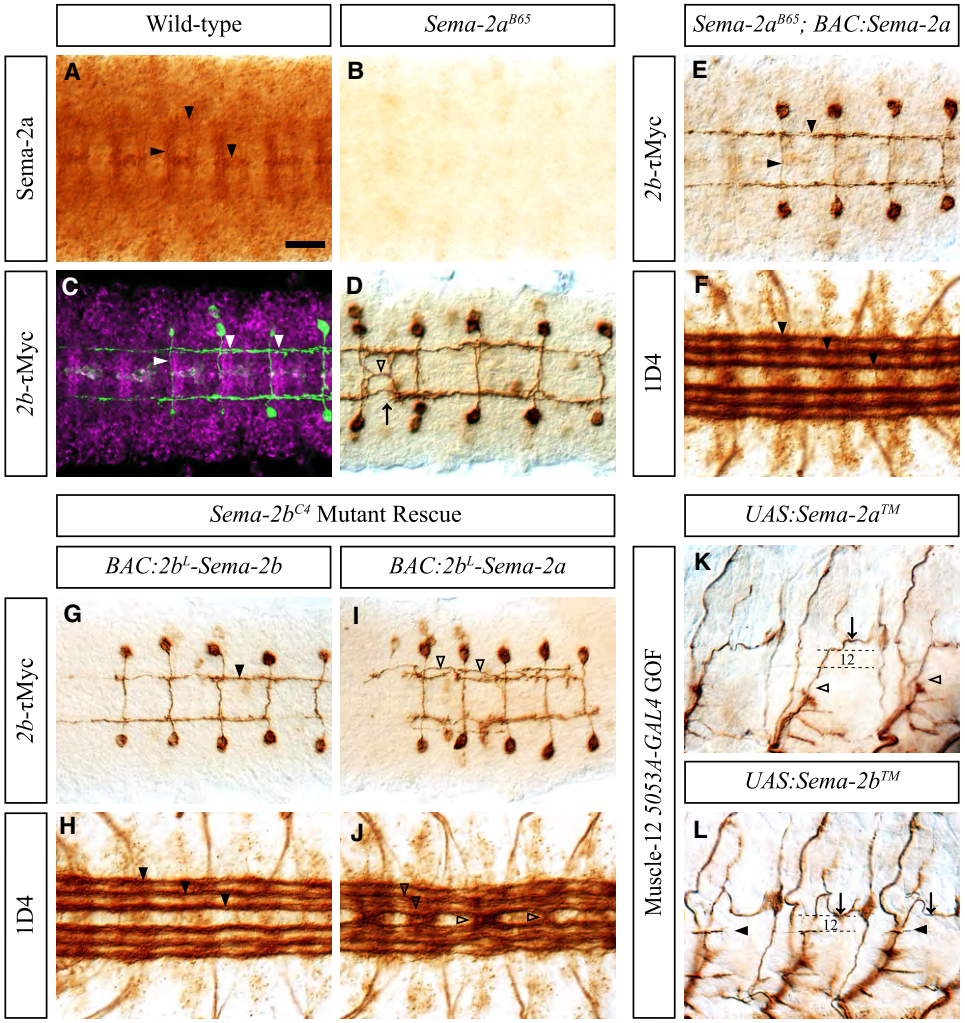

Figure 4. Sema-2a Is Broadly Distributed in the Embryonic CNS and, Unlike Sema2b, Functions as an Axonal Repellent to Position Longitudinal Tracts

(A) Wild-type embryos stained with the anti-Sema-2a mAb 19C2. Sema-2a protein is distributed along the CNS midline, commissural axons, and more diffusely along longitudinal tracts (arrowheads).

(B) Sema-2a protein is undetectable in *Sema-2a*^{B65} null mutant embryos.

(C) *2b-τMyc* axons navigate along CNS regions that contain lower Sema-2a expression levels (arrowheads).

(D) In *Sema-2a*^{B65} mutant embryos, *2b-τMyc* axons often detour medially (arrows), sometimes crossing the CNS midline (empty arrowhead, see Figure 5H for quantification).

(E and F) The *BAC:Sema-2a* transgene, which includes the *Sema-2a* genomic region, fully rescues *2b-τMyc* pathway defects (E) and 1D4-i tract formation (F) in *Sema-2a*^{B65} null mutants.

(G–J) Sema-2a and Sema-2b function differently when expressed under the control of the *Sema-2b*^{L} promoter. (K and L) Sema-2a^{TM} repels, whereas Sema-2b^{TM} attracts, motor neuron axons when overexpressed on peripheral muscle-12 (dashed lines: dorsal and ventral boundaries of muscle 12). Scale bar in (A) represents: 16 μm (A–J); 20 μm (K–L). See also Figure S4.

lateral branches of the SNa pathway, which were observed to retain ectopic contact with muscle-12 in ~30% of hemisegments, a phenotype never observed in wild-type embryos (Figure 4L, arrows, and Figures S4D and S4E). Overexpression of Sema-2a^{TM} from the same muscle had no effect on SNa motor axons (Figure 4K, arrows, and Figure S4D), further demonstrating that Sema-2a and Sema-2b mediate distinct guidance functions.

Taken together, these GOF experiments demonstrate that Sema-2a and Sema-2b function differently in both CNS longitudinal connectives and motor axons: Sema-2b functions to promote axonal attraction, whereas Sema-2a functions as a repellent.

Neuronal Cell-Type Autonomous Requirements for PlexB in Longitudinal Tract and Sensory Afferent Targeting in the CNS

To understand how PlexB mediates secreted semaphorin signaling during CNS development, we first examined its

requirement for *2b-τMyc* pathway formation. In *PlexB*$^{-/-}$ mutant embryos the *2b-τMyc* pathway formation is severely disrupted; *2b-τMyc* longitudinally projecting axons are often defasciculated, and individual axons are diverted both medially and laterally (Figures 5A and 5H). This phenotype is a combination of both the *Sema-2a*$^{-/-}$ and *Sema-2b*$^{-/-}$ mutant phenotypes (Figures 5G and 5H). Using the *elav-GAL4* driver to express PlexB in all neurons in the *PlexB*$^{-/-}$ mutant, we observed full rescue of the *2b-τMyc* pathway (Figure 5B) and also full rescue, as previously reported (Ayoob et al., 2006), of the adjacent 1D4-i tract (Figure 5C). These data further support PlexB functioning to integrate both Sema-2a-mediated repulsion and Sema-2b-mediated attraction, resulting in proper organization of select CNS longitudinal tracts.

PlexB is enriched in the intermediate and lateral regions of the CNS scaffold (Figures S5A–S5C). To determine in which neurons PlexB functions, we next assessed the requirement for PlexB in distinct neuronal populations. In a wild-type background, pan-neuronal overexpression, using the *elav-GAL4* driver of a modified PlexB receptor lacking its cytoplasmic domain (PlexB^{EcTM}) leads to the disorganization of both the *2b-τMyc* pathway and the 1D4-i tract (Figure 5D), phenocopying the *PlexB*$^{-/-}$ null mutant and showing that PlexB^{EcTM} functions as a dominant-negative receptor. The MP1 neurons, which can be genetically labeled by the *sim-GAL4* driver (Hulsmeier et al., 2007), serve as pioneer axons for the 1D4-i tract (Figures S5D–S5F) (Hidalgo and Brand, 1997). The MP1 longitudinal pathway resides in the same intermediate region as the *2b-τMyc* pathway and lies directly adjacent to it (Figures S5G–S5I). Expressing PlexB^{EcTM} selectively in these neurons disrupts 1D4-i tract formation; however, the *2b-τMyc* pathway remains intact (Figure 5E and Figures S5J–S5L). A similar neuronal cell-type autonomous requirement for PlexB was apparent after PlexB^{EcTM} overexpression solely in ch neurons under control of the *iav-Gal4* driver. We observed disruption of ch axon targeting within the CNS similar to what we observe in *PlexB*$^{-/-}$ mutants (Figure 5F) even though CNS longitudinal pathways in *iav-GAL4, UAS: PlexB*^{EcTM} embryos remain intact. Importantly, overexpression of full length PlexB using the same *iav-GAL4* driver leads to no such phenotype in ch afferent targeting (data not shown). These results indicate that PlexB function is autonomously required in both central and peripheral neurons for correct patterning of their projections within the intermediate domain of the neuropile, presumably through recognition and integration of both Sema-2b attraction and Sema-2a repulsion. By directing the projections of both sensory afferents and CNS interneurons to the same narrow region of the neuropile, PlexB allows for correct synaptic connections and circuit formation between ch axons and their CNS postsynaptic partners.

Ch Sensory Afferent Targeting within the CNS Requires Secreted Semaphorins

To determine how Sema-2a and Sema-2b directly regulate PlexB-mediated CNS targeting of ch sensory afferents, we analyzed ch CNS targeting in *Sema-2a*$^{-/-}$, *Sema-2b*$^{-/-}$, and *Sema-2a*$^{-/-}$,*Sema-2b*$^{-/-}$ double null mutant embryos. In *Sema-2a*^{B65} null mutant embryos, ch axon terminals within the CNS still exhibit longitudinally continuous branches along the lateral extent of the 1D4-i tract; in addition, some ch axons display ectopic projections medially (Figures 6A–6C, 6J, and 6K; quantification in Figures S6A–S6F). In the *Sema-2b*^{C4} null mutants, however, ch axons fail to elaborate their characteristic morphology within the CNS, most often terminating in a position that is lateral to the location where the 1D4-i connective normally forms and failing to form a continuous longitudinal branch between segments (Figures 6D–6F, 6J, and 6K; quantification in Figures S6A–S6F). In *Sema-2ab*^{A15} double null mutants, ch axons project within the CNS in a zone that includes the intermediate longitudinal region; however, terminal branches are completely disorganized (Figures 6G–6K; quantification in Figures S6A–S6F), exhibiting both ectopic lateral and medial projections as they do in *PlexB*$^{-/-}$ mutants (Figures 1H and 6J). These results support PlexB-Sema-2b signaling acting to attract extending axons to the intermediate longitudinal region of the neuropile, whereas Sema-2a acts as a repellent; both ligands utilize the same receptor and act in concert to ensure the accurate assembly of sensory afferents with correct CNS connectives (Figure 6L).

Normal Larval Responses to Vibration Require Precise ch Sensory Afferent Targeting within the CNS

Our genetic analyses show that PlexB-Sema-2b signaling is critical for correct ch afferent innervation and CNS interneuron projections within the same intermediate region of the embryonic CNS. Termination of sensory afferents and their putative postsynaptic partners within the same narrow region of the neuropile may be necessary for proper synaptic connection and circuit assembly. Therefore, we next asked whether functional consequences result from the neuronal wiring defects we observe following disruption of Sema-2b-PlexB signaling.

Ch neurons in the *Drosophila* adult have been implicated as mechanosensory transducers for acoustic signals (Eberl, 1999), and also are presumed to be involved in larval proprioception and mechanosensation (Caldwell et al., 2003). To assess larval ch sensory neuron functions in a high throughput manner, we developed an assay for larval vibration sensation. Approximately 100 larvae were placed on a large agar-filled dish located above a loud speaker. We used the Multi-Worm Tracker (MWT) software (http://sourceforge.net) (Swierczek N., Giles A., Rankin C. and Kerr R., unpublished data) to automatically deliver vibration stimuli with the speaker while tracking the entire larval population on the dish. Prior to the onset of vibration larvae engage in normal foraging behavior, mostly crawling straight and occasionally making turns. We found that vibration induces a stopping response, followed by head turning (Figures 7A and 7A′; Movies S1 and S2). Larval head turning in response to vibration is highly reproducible and readily quantifiable using the MWT software (Figures 7B and 7E). This "startle" reaction to mechanical stimuli may allow the larva to sample its environment and change crawling direction following detection of potentially harmful stimuli.

We found that *atonal* (*ato*^{1}) mutant larvae, which lack ch neurons (Jarman et al., 1993), do not exhibit a normal response to vibration. Upon stimulation, they show a small decrease in crawling speed (data not shown) with no head turning (Figures 7C and 7E). We inhibited synaptic transmission in ch neurons

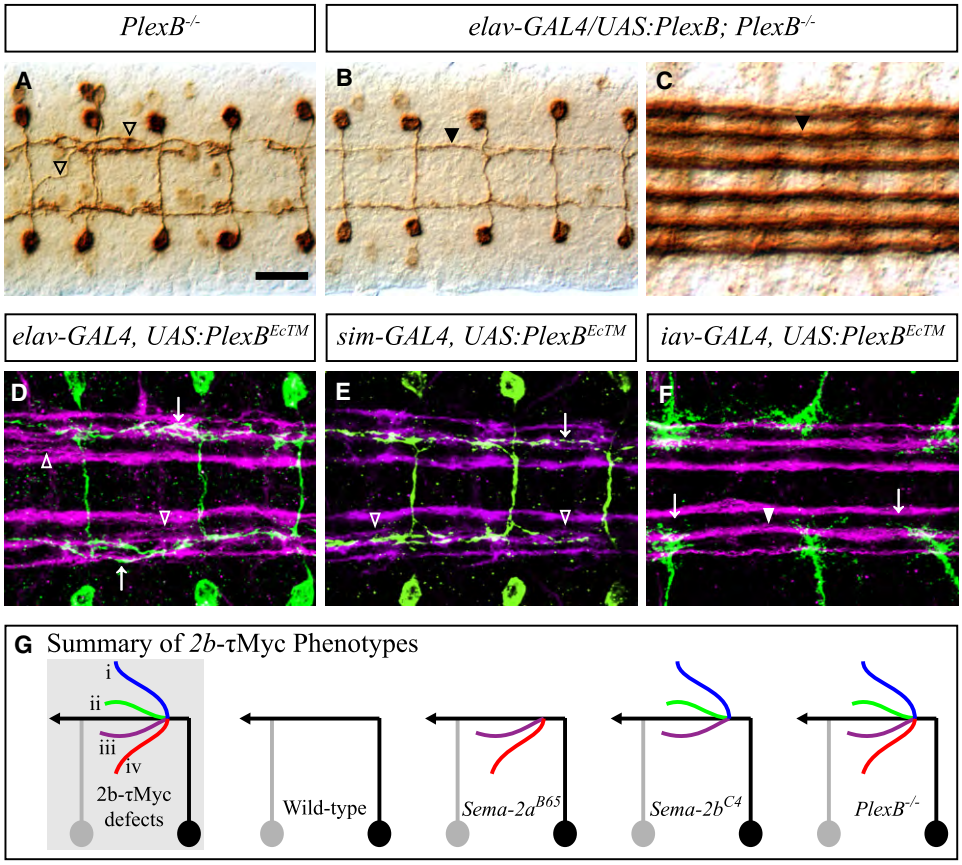

H *2b*-τMyc^{+} Longitudinal Pathway Defect Quantification

Genotype	*2b* -τMyc longitudinal pathway defects per embryo				Counted Embryos
	^{i}Lateral Exit	^{ii}Lateral Detour	^{iii}Medial Detour	^{iv}Midline Crossing	
Wild-type	**0**	**0**	**0**	**0**	*92*
Sema-2a ^{B65}	**0**	**0**	**0.67**	**0.30**	*81*
Sema-2a ^{B65} *; BAC:Sema-2a*	0	0	0.03	0	*70*
Sema-2b ^{C4}	**0.61**	**2.54**	**0.73**	**0**	*41*
Sema-2b ^{C4} *; BAC:Sema-2b*	0.05	0.36	0.14	0	*22*
Sema-2b ^{C4} *; BAC:Sema-2b* ^{TM}	0.38	0.92	0.33	0	*24*
Sema-2b ^{C4} *; BAC:2b* ^{L} *-Sema-2a*	0.53	3.47	0.53	0	*17*
Sema-2b ^{C4} *; BAC:2b* ^{L} *-Sema-2b*	0.18	0.57	0.18	0	*28*
PlexB $^{-/-}$	**0.47**	**2.93**	**2.13**	**0.50**	*30*
elav-GAL4/UAS:PlexB; PlexB $^{-/-}$	0	0.07	0	0	*14*

Figure 5. Neuronal PlexB Mediates the Organization of Both CNS Longitudinal Connectives and ch Sensory Afferent CNS Projections

(A) The *2b-τMyc* longitudinal projecting axons are defasciculated, and they often detour laterally and cross the CNS midline in *PlexB*$^{-/-}$ mutant embryos (empty arrowheads). Scale bar in (A) represents 10 μm (A–F).

(B and C) *elav-GAL4* pan-neuronal expression of full-length PlexB fully rescues formation of the 2b-τMyc^{+} pathway (B) and 1D4-m longitudinal tract (C) in *PlexB*$^{-/-}$ mutants.

(D–F) Disruption of endogenous PlexB signaling in different neuronal pathways. (D) Both *2b-τMyc* and 1D4-m pathways are disorganized and defasciculated when PlexB^{EcTM} is expressed under the pan-neuronal driver *elav-GAL4*. (E) The 1D4-m connective, but not the *2b-τMyc* pathway, is disrupted when PlexB^{EcTM} is expressed in MP1 neurons using the *sim-GAL4* driver (see also Figure S5J). (F) *UAS:PlexB*^{EcTM} expression in ch axons using the *iav-GAL4* driver abolishes normal CNS targeting of ch axons and phenocopies defects observed in *PlexB*$^{-/-}$ mutants.

by combining the *iav-GAL4* with *UAS-TNT* (tetanus toxin) and found that *iav-TNT* larvae, which have inactivated ch neurons, do not show significant increases in head turning in response to vibration as compared to control larvae that express GFP (*iav-GFP*) in ch neurons (Figures S7A, S7B, and S7D). Therefore, ch neurons are a major class of larval sensory neurons involved in sensing vibration, and their proper synaptic input to the CNS is required for inducing normal head turning behavior in response to vibration.

In *Sema-2b*^{C4} mutant larvae we also observed an abnormal response to vibration. *Sema-2b*^{C4} mutant larvae do reduce their speed significantly in response to vibration (data not shown), however they show no head turning (Figures 7D and 7E), similar to the vibration responses observed in *ato*^{1} mutant larvae. These results suggest that defective larval vibration responses observed in the absence of *Sema-2b* result from ch neurons being unable to establish appropriate sensory afferent connectivity within the CNS (Figure 6F).

The behavioral deficits observed in *Sema-2b*^{C4} null mutant larvae could also be contributed by requirements for Sema-2b-PlexB signaling in other neuronal populations that are part of the circuitry essential for vibration responses. Therefore, we genetically manipulated PlexB signaling solely in ch neurons. As shown above (Figure 5F), expressing a dominant-negative PlexB receptor selectively in ch neurons (*iav-PlexB*^{EcTM}) severely disrupts CNS targeting of ch sensory afferents. We found that the response to vibration in *iav-PlexB*^{EcTM} larvae is severely compromised as compared to control larvae that express GFP (*iav-GFP*) in ch neurons (Figure 7E, see trace in Figure S7C), similar to the head-turning deficit we observe in *ato*^{1}, *iav-TNT*, and *Sema-2b*^{C4} mutant larvae. This indicates that the proper targeting of ch afferent innervation in CNS is indeed important for normal larval vibration behavior. Therefore, PlexB-mediated signaling regulates normal targeting and elaboration both of ch afferent synaptic input and interneuron connective assembly in the same target area, thereby ensuring correct assembly of circuitry involved in processing ch sensory information and generating appropriate responses to vibration.

DISCUSSION

A Semaphorin-Plexin Code Functions Together with the Slit-Robo Code to Assemble CNS Neural Circuits

The establishment of CNS longitudinal tracts in *Drosophila* occurs sequentially, from medial to lateral, through a series of distinct guidance events. These include extension of processes that pioneer these trajectories, and subsequent fasciculation and defasciculation events that allow additional processes to join these pathways, cross segment boundaries, and establish connectives that span the rostrocaudal axis of the embryonic CNS (Hidalgo and Booth, 2000). During this process, a repulsive Slit gradient acts over a long range to establish three distinct lateral regions for longitudinally projecting axons, the choice of which is determined by differential expression of Robo receptors (Dickson and Zou, 2010). Once they settle within an appropriate lateral region, individual axons that are part of the same bundle must then adhere to one another and remain fasciculated. We find that Sema-2b signals through PlexB to accomplish this task for longitudinal connectives in the intermediate region.

Interestingly, this Sema-2b-PlexB-mediated organization is inherently connected to Slit-Robo-mediated patterning. The lateral position of intermediate longitudinal processes, including the *2b-τMyc* pathway, is initially determined by Robo3-mediated signaling (Evans and Bashaw, 2010; Rajagopalan et al., 2000; Simpson et al., 2000; Spitzweck et al., 2010). Therefore where Sema-2b is expressed reflects lateral positional information derived from the Robo code. Then, this lateral information is further conveyed by the continuous Sema-2b expression over the entire anterior/posterior axis, mediating local organization of both CNS interneurons and sensory afferent projections through the PlexB receptor. When PlexB signaling is disrupted, *2b-τMyc* axons still project across the CNS midline and turn rostrally at the appropriate medial-to-lateral position; however, they subsequently wander both medially and laterally, often crossing the medio-lateral regional boundaries set by the Robo code (Figure 5G). Therefore, PlexB-mediated Sema-2b signaling solidifies specific projection positioning originally established by the Robo code. Together, these two distinct Robo and plexin guidance cue signaling modules function in a sequential and complementary fashion to specify both long range medial-to-lateral positioning (Robo) and short-range local fasciculation (PlexB). PlexA, the other *Drosophila* plexin receptor, and its ligand Sema-1a are specifically required for the proper formation of the 1D4-l pathway (Winberg et al., 1998b; Yu et al., 1998). However, Sema-1a does not show restricted expression within the medio-lateral axis of the nerve cord analogous to that observed for Sema-2b (Yu et al., 1998), suggesting a different mechanism may underlie Sema-1a–PlexA regulation of fasciculation in the most lateral CNS longitudinal region.

Following medio-lateral specification by Slit-Robo signaling and general organization of longitudinal regions by Sema-plexin signaling, additional cues are likely to mediate local interactions among neural processes already restricted to defined regions in the neuropile. Several cell surface proteins may serve such functions; for example, the cell adhesion molecule (CAM) connectin, like Sema-2b, shows exquisitely restricted expression along a subset of longitudinal projections (Nose et al., 1992). More widely expressed CAMs also play important roles in maintaining the fasciculated state of longitudinally projecting processes that are part of the same connective; indeed, in the absence of the *Drosophila* Ig super family member FasII, axons that contribute to the MP1 pathway show reduced association when examined at high resolution (Lin et al., 1994). Therefore, an ensemble of short-range cues expressed in distinct subsets of longitudinally projecting neurons allows for individual pathways to be established following more global restriction to appropriate locations, and as we demonstrate here, this process is critical for the neural circuit function. It seems likely that similar mechanisms underlie

(G) Summary of *2b-τMyc* pathway phenotypes in the genetic backgrounds assessed in this study. *2b-τMyc* pathway defects were binned into four categories: (i) lateral exit; (ii) lateral detour; (iii) medial detour; and (iv) midline crossing.
(H) Quantification of the number of *2b-τMyc* defects/embryo in all genotypes examined (null mutants indicated in bold). See also Figure S5.

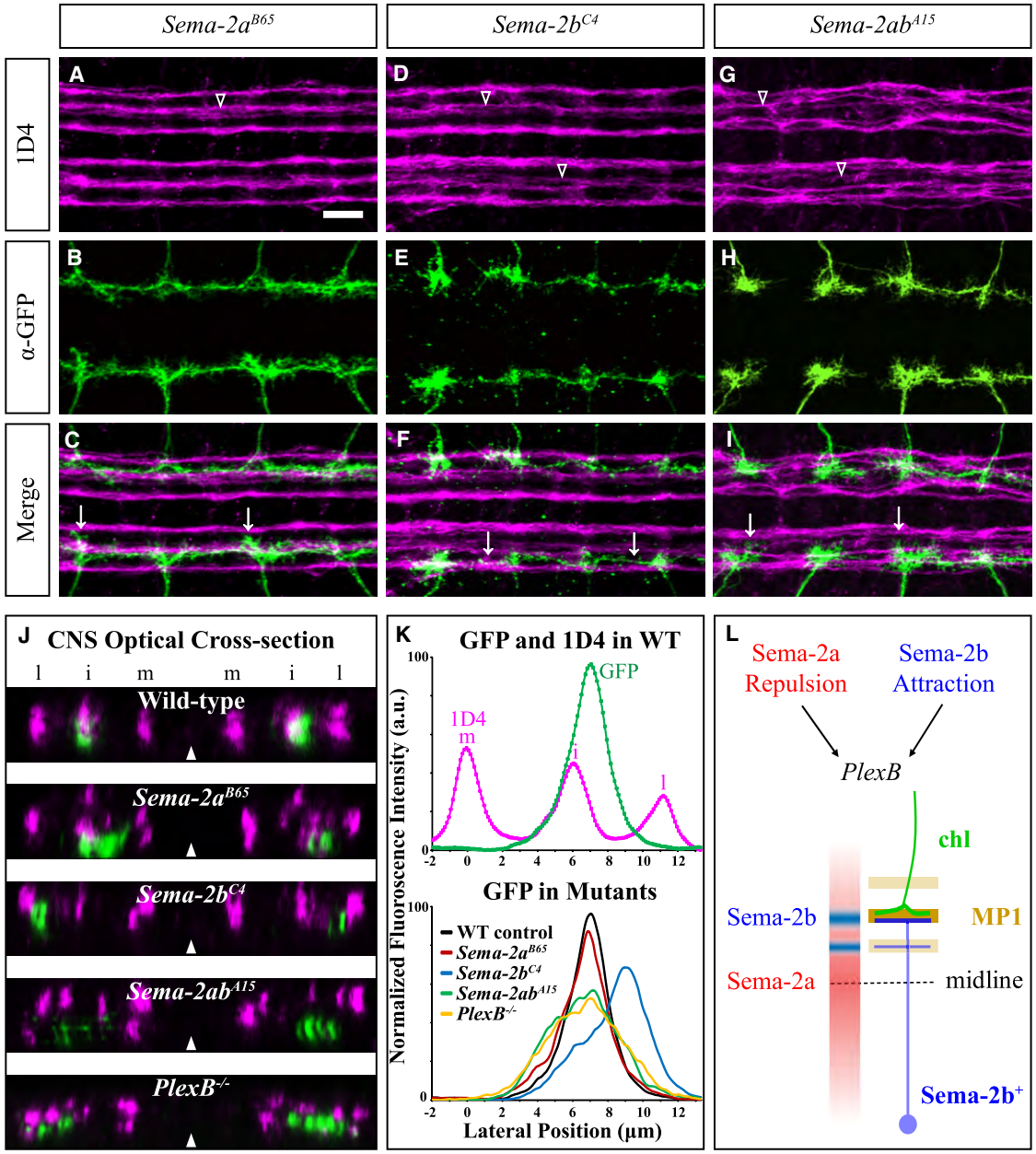

Figure 6. Sema-2a and Sema-2b Cooperate to Ensure Correct Targeting of ch Sensory Afferent Projections within the CNS

(A–I) Ch axon CNS projections revealed using the *iav-GAL4/UAS:syt-GFP* marker in late stage-16 *Sema-2a*^{B65} mutant embryos (A–C), *Sema-2b*^{C4} mutants (D–F), or *Sema-2a/Sema-2b* double mutants (G–I). Scale bar in (A) represents 10 μm (A–I); 3.5 μm (J).

(J) Optical cross-sections through the CNS of different genetic backgrounds provide a coronal view of both ch afferent projections and 1D4^{+} longitudinal connectives.

(K) Quantification of ch afferent targeting phenotypes in different genetic backgrounds. 1D4 and GFP signal profiles were plotted along the medial-to-lateral axis (see Experimental Procedures for quantification methods and Figure S6 for additional quantification).

(L) Schematic showing PlexB integration of both Sema-2a repulsion and Sema-2b attraction to promote the assembly of CNS longitudinal tracts and ch sensory afferent targeting within the CNS. See also Figure S6.

the segregation of complex trajectories, the establishment of laminar organization, and the formation of discrete neural maps in other regions of invertebrate and vertebrate nervous systems (Matsuoka et al., 2011; Sanes and Yamagata, 2009).

Plexin B Mediates Both Sema-2b Attraction and Sema-2a Repulsion

Our analyses allow for a comparison between the effects of the secreted semaphorins Sema-2a and Sema-2b on both CNS

interneuron trajectories and sensory afferent targeting within the CNS. We observed in both LOF and GOF genetic paradigms that Sema-2a acts as a repellent, consistent with previous observations (Ayoob et al., 2006; Bates and Whitington, 2007; Carrillo et al., 2010; Matthes et al., 1995; Winberg et al., 1998a; Zlatic et al., 2009). Sema-2b, in contrast, serves an opposite guidance function and promotes neurite fasciculation. The highly restricted expression of Sema-2b within the intermediate domain of the nerve cord serves to assemble select longitudinal tracts and ch sensory afferents in this region, strongly suggesting that Sema-2b functions as a local attractive cue to define a specific CNS subregion and influence the organization of specific circuits.

Although both Sema-2b and Sema-2a signal through the same receptor, PlexB, they appear to do so independently. In the absence of Sema-2a, Sema-2b is still required for fasciculation and organization of the *2b-τMyc* and 1D4-i tracks, and also for correct ch afferent innervation in the intermediate region of the nerve cord. In the absence of Sema-2b, Sema-2a expression alone results in potent repellent effects within the CNS for both the *2b-τMyc* pathway and ch sensory afferent targeting. The distinct attractive and repulsive functions of Sema-2b and Sema-2a, respectively, are further revealed by the different phenotypes observed in GOF experiments. In the CNS of *Sema-2b*$^{-/-}$ mutant embryos, expression of Sema-2a under the control of the *Sema-2b* promoter results in both *2b-τMyc* and 1D4^{+} tract defasciculation much more severe than what is observed in the *Sema-2b* mutant alone; similar expression of Sema-2b fully rescues the discontinuous and disorganized *Sema-2b*$^{-/-}$ longitudinal connective phenotypes. Moreover, membrane-tethered Sema-2b is similarly capable of rescuing the *Sema-2b*$^{-/-}$ mutant phenotype, further supporting the idea that Sema-2b is a short-range attractant. In the periphery, misexpression of transmembrane versions of both Sema-2b and Sema-2a in a single body wall muscle demonstrates that Sema-2b™ overexpression results in motor neuron attraction, whereas Sema-2a™ in this same misexpression paradigm functions as a motor axon repellent.

We also show that PlexB is the receptor that mediates both Sema-2a and Sema-2b functions in the intermediate region of the developing nerve cord. Only *Sema-2a*$^{-/-}$, *Sema-2b*$^{-/-}$ double null mutants, and not either single mutant, fully recapitulates the *PlexB*$^{-/-}$ mutant phenotype, and ligand binding experiments demonstrate that PlexB is the endogenous receptor for both Sema-2a and Sema-2b in the embryonic nerve cord. However, both ligands exert opposing guidance functions despite sharing over 68% amino acid identity and also very similar protein structures (R. Robinson, Z.W., A.K., and Y. Jones, data not shown). In vertebrates, distinct plexin coreceptors often bias the sign of semaphorin-mediated guidance events (Bellon et al., 2010; reviewed by Mann et al., 2007). We find that the *Drosophila* ortholog of Off-Track, a transmembrane protein implicated in modulation of vertebrate and invertebrate plexin signaling (Toyofuku et al., 2008; Winberg et al., 2001), apparently does not function in the *Drosophila* PlexB-mediated guidance events investigated here (data not shown). It will be important to define the relevant differences between the Sema-2a and Sema-2b proteins that are critical for affecting divergent PlexB signaling, and whether or not unique ligand-receptor protein-protein interactions result in differential PlexB activation of signaling cascades with diametrically opposed effects on cytoskeletal components (Hu et al., 2001).

Semaphorin-Mediated Sensory Afferent Targeting within the CNS

We find here that Sema-plexin signaling critical for specifying a subset of intermediate longitudinal pathways is also utilized to generate precise mapping of ch sensory input onto CNS neurons. In *Drosophila*, different classes of sensory axons target to distinct regions of the nerve cord neuropile (Merritt and Whitington, 1995), and the same Robo code essential for positioning CNS axons also regulates the medio-lateral positioning of sensory axons within the CNS (Zlatic et al., 2003; Zlatic et al., 2009). In addition to slit-mediated repulsive effects on sensory afferent targeting, Sema-1a and Sema-2a also restrict the ventrally and medially projecting afferents of the pain sensing Class IV neurons within the most ventral and most medial portions of the nerve cord neuropile (Zlatic et al., 2009). This is reminiscent of recent observations in the mammalian spinal cord showing that a localized source of secreted Sema3e directs proprioceptive sensory input through plexin D1 signaling, ensuring the specificity of sensory-motor circuitry in the spinal cord through repellent signaling (Pecho-Vrieseling et al., 2009). In addition, the transmembrane semaphorins Sema-6C and 6D provide repulsive signals in the dorsal spinal cord that direct appropriate proprioceptive sensory afferent central projections (Yoshida et al., 2006). However, little is known about the identity of cues that serve to promote selective association between sensory afferents and their appropriate central targets in vertebrates or invertebrates. We find that PlexB signaling guides ch sensory terminals to their target region in the CNS through Sema-2b-mediated attraction. Selective disruption of PlexB function in ch neurons severely abolishes normal ch afferent projection in the CNS. Using a high-throughput assay for quantifying larval behavioral responses to vibration, we confirm a role for ch sensory neurons in larval mechanosensation (Caldwell et al., 2003). Using this assay we are also able to show that precise ch afferent targeting is required for central processing of vibration sensation and subsequent initiation of appropriate behavioral output. At present, we do not know the precise postsynaptic target of ch axons, though our analysis suggests the Sema-2b^{+} neurons are good candidates. Combining vibration response assays with visualization of activated constituents of the ch vibration sensation circuit will allow for a comprehensive determination of input and output following proprioceptive sensation.

Common Molecular Mechanisms Underlying Sequential Organization of Interneuron and Sensory Afferent CNS Connectivity

The formation of a functional circuit relies on the precise assembly of a series of pre- and postsynaptic components. Robo3-mediated signaling is required both for the targeting of ch axons and a subset of the longitudinally projecting interneurons to the same broad intermediate domain of the neuropile (Zlatic et al., 2003). We show here that PlexB-mediated signaling

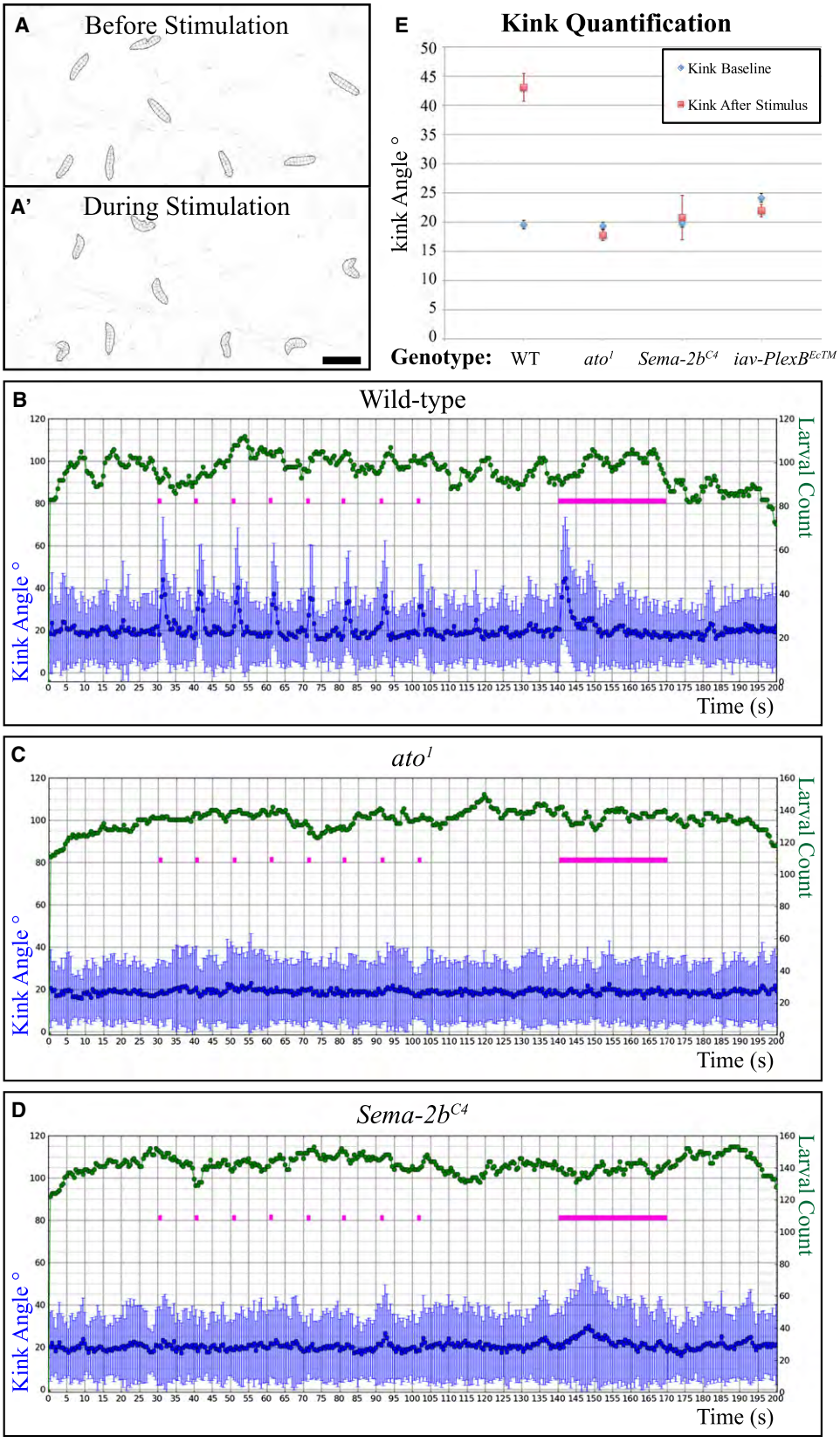
A
Before Stimulation
A'
During Stimulation
E
Kink Quantification
Kink Baseline
Kink After Stimulus
kink Angle °
Genotype: WT ato1 Sema-2bC4 iav-PlexBEcTM
B
Wild-type
C
ato1
D
Sema-2bC4
Kink Angle °
Larval Count
Time (s)

is important for both the assembly of distinct longitudinal projections and also the targeting of ch sensory axon terminal arborizations within the same restricted subregion of the Robo3-defined intermediate domain of the *Drosophila* embryonic nerve cord. We find that the secreted semaphorin Sema-2b is a PlexB ligand that plays a central role in both of these guidance events during *Drosophila* neural development. Sema-2b-PlexB signaling promotes selective fasciculation of the small population of longitudinally projecting axons that express Sema-2b and also immediately adjacent longitudinal projections in the intermediate medio-lateral region of the development CNS. Sema-2b also facilitates targeting of ch afferent terminals that subsequently arrive and establish synaptic contacts in this intermediate region of the developing nerve cord. Sema-2b-PlexB signaling ensures the correct assembly of the circuit that processes ch sensory information, and in its absence larval vibration responses are dramatically compromised. Interestingly, the other PlexB ligand within the CNS, Sema-2a, plays an opposing role to Sema-2b by preventing aberrant targeting through repulsion; together, these two secreted semaphorin ligands act in concert to assure precise neural projection in the developing CNS. Therefore, a combinatorial guidance code utilizes both repulsive and attractive semaphorin cues to mediate the accurate connection of distinct CNS structures and, ultimately, to ensure functional neural circuit assembly.

EXPERIMENTAL PROCEDURES

Generation of Transgenes

From large *Drosophila* BAC clones (RPCI-98: BACPAC resource at CHORI, see clone coordinates in Figure S2A), genomic fragments containing *Sema-2b* (CG33960, FlyBase) or *Sema-2a* (CG4700) were retrieved by gap-repair into the attB-P[acman]-ApR vector; constructs were then integrated into engineered attP landing sites in *Drosophila* (Venken et al., 2006). For *Sema-2b* promoter ($2b^L$) BAC transgenes, a ~35 Kb genomic fragment upstream from the *Sema-2b* protein coding sequence was used to drive the expression of τGFP, Sema-2a, or Sema-2b. The Sema-2b coding sequence was subcloned from a cDNA construct (a gift from B. Dickson, Institute of Molecular Biotechnology of the Austrian Academy of Sciences) corresponding to M_{49}-V_{784} in the ACL83134 (Genbank) protein sequence. For membrane-tethered modification of Sema-2a and Sema-2b in pUASt constructs or BAC constructs, the TM-GFP region of the mCD8-GFP protein (Lee and Luo, 1999) was cloned in frame to the C terminus of these secreted semaphorins. To generate $PlexB^{EcTM}$, the entire extracellular and transmembrane regions (1468 aa in total) of the Myc-PlexB protein (Ayoob et al., 2006), followed by a stop codon, were subcloned into the pUASt vector.

Genetic Analyses

To generate *Sema-2a* and *Sema-2b* null alleles, genomic deletions were made using Flippase recognition target (FRT) sites (Parks et al., 2004) to remove *Sema-2a* (*FDD-000938: Sema2a*^{B65}), *Sema-2b* (*FDD-0012943: Sema-2b*^{C4}), or *Sema-2a* and *Sema-2b* (*FDD-0012939: Sema-2ab*^{A15}) (see deleted regions, Figure S2A). All other mutant stocks have been previously described: $plexB^{KG00878}$ (Ayoob et al., 2006), $Sema\text{-}1a^{P1}$ (Yu et al., 1998), and $plexA^{Df(4)C3}$ (Winberg et al., 1998b). Specific GAL4 drivers were used to label and manipulate particular subsets of neurons and their projections, including: *iav-GAL4* (gift of C. Montell, Johns Hopkins University) for chordotonal sensory neurons, and *sim-GAL4* (Hulsmeier et al., 2007) for MP1 neurons. Other GAL4 drivers used were *elav-GAL4* (Yao and White, 1994) and *5053A-GAL4* (Swan et al., 2004). The *2b-τMyc* pathway was labeled with the *Sema2b-τMyc* marker (Rajagopalan et al., 2000). For overexpression studies, the following UAS transgenes were used: *UAS:Sema-2a-TM-GFP*, *UAS:Sema-2b-TM-GFP*, and $UAS{:}myc\text{-}plexB^{EcTM}$ (this work); *UAS:myc-plexB* (Ayoob et al., 2006), *UAS:syt-GFP* (Bloomington Stock Center #6926).

Immunohistochemical Analyses

Embryo collections and stainings were performed as described (Ayoob et al., 2006; Yu et al., 1998) using the following primary antibodies: anti-Fas II mAb 1D4, (1:4; Vactor et al., 1993), anti-Sema-2a mAb 19C2 (1:4; Winberg et al., 1998a), rabbit polyclonal anti-Sema-2b (1:1000; L.B.S., Y. Chou, Z.W., T. Komiyama, C.J. Potter, A.L.K., K.C. Garcia, and L.L., unpublished data), rabbit anti-GFP (1:1000, Molecular Probes), anti-Myc mAb 9E10 (1:1000, Sigma), anti-Myc mAb 71D10 (1:1000, Cell Signaling), and rabbit anti-Tau (1:200, AnaApec). Rabbit anti-PlexB antibody was generated by New England Peptide according to the peptide sequence CRYKNEYDRKKRRADFGD in the extracellular domain of the PlexB protein, custom affinity purified and used at 1:200. HRP-conjugated goat anti-mouse and anti-rabbit IgG/M (1:500, Jackson Immunoresearch), Alexa488 or Alexa546-conjugated goat anti-mouse IgG, and Alexa647-conjugated goat anti-rabbit IgG (1:500, Molecular Probes) were used as secondary antibodies. Embryos at select developmental stages were dissected to reveal the CNS from the dorsal side, and images were acquired as described (Ayoob et al., 2006) or using a Zeiss LSM 510 confocal microscope.

Quantification of the 1D4-i Tract Defects

To quantify 1D4-i tract defects, the CNS region of dissected embryos was observed from the dorsal side at 40× under bright-field. T2, T3, and A1-8 segments were included for analysis from each embryo. The measure of 1D4-i trajectory disorganization was whether or not two or more $1D4^+$ bundles in the intermediate region of the longitudinal connectives were observed to have a separation of more than one wild-type $1D4^+$ bundle width; if so, the

Figure 7. Normal Larval Responses to Vibration Require Precise ch Sensory Afferent Targeting within the CNS

(A and A′) Two still schematic images from a movie (see Movie S1) showing contours and skeletons of *Drosophila* larvae before and during the vibration stimulus. Vibration induces stopping, followed by head turning ("kink"). Scale bar in (A′) represents 5 mm (A, A′).

(B–D) Ch neurons and Sema-2b are required for normal larval response to vibration. Graphs show mean head turning angle (in degrees) as a function of time for wild-type (*w1118*), ato^1, and $Sema\text{-}2b^{C4}$ mutant larvae. Green dots (upper trace) show number of larvae tracked by the software within each 0.5 s interval. Vibration stimuli are indicated by the red bars. Blue dots (lower trace) show mean absolute kink angle; blue error bars show standard deviation from the mean angle (see Figure S7 for more details). (B) Wild-type larvae react to vibration by stopping and turning their heads. Note the marked increase in mean angle after each vibration stimulus. (C) ato^1 mutant larvae, which lack ch neurons, do not turn in response to vibration. (D) $Sema\text{-}2b^{C4}$ mutant larvae do not turn in response to vibration.

(E) Quantification of head turning in response to vibration of wild-type, ato^1, $Sema\text{-}2b^{C4}$, and $iav\text{-}PlexB^{EcTM}$ larvae. Blue marks show mean angle before stimulus as baseline values. Blue error bars show standard errors of the mean relative baseline values. Red marks show mean angle of larvae during the presentation of vibration stimulus. Red error bars show standard errors of the mean angle during vibration. During vibration, wild-type larvae exhibit significant increases in turning compared to the baseline ($p < 0.001$; Student's t test). Although they have similar baseline turning values, ato^1, $Sema\text{-}2b^{C4}$, and $iav\text{-}PlexB^{EcTM}$ mutant larvae do not show significant increases in turning in response to vibration compared to wild-type ($p < 0.001$, Student's t test).

Scale bar in A′: 5mm for A and A′.

See also Figure S7 and Movies S1 and S2.

hemisegment was scored as disorganized. This determination was made halfway between adjacent ISN nerve roots for each segment scored.

Alkaline Phosphatase-Binding Assays

The binding of alkaline phosphatase (AP)-tagged ligands to *Drosophila* S2R+ cells, or to dissected embryonic ventral nerve cords, was assessed as described (Ayoob et al., 2006; Fox and Zinn, 2005). To select live *plexB*$^{-/-}$ mutant embryos, the *plexB* ^{KG00878} allele was placed over a fourth chromosome GFP marker (a gift from B. McCabe, Columbia University). Homozygous mutant embryos were then identified by their lack of GFP fluorescence using a Zeiss LUMAR.V12 fluorescent stereoscope. To produce AP-ligands, Sema-2a or Sema-2b cDNAs were cloned into the APtag-5 vector (GenHunter) using NheI and BglII sites. The entire DNA fragment expressing secreted Sema-2a-AP, or Sema-2b-AP fusion protein ligand, was subcloned to the pUASt vector using NotI and XbaI sites. The pUASt constructs were cotransfected with an Act-GAL4 plasmid into S2R+ cells cultured in a serum-free Schneider's *Drosophila* medium (1×, GIBCO). Four days after transfection, the cell culture supernatants were collected and concentrated. Freshly prepared ligands were used each time, and ligand quality was assessed using western blot. Ligand concentrations were measured by quantifying AP activity, and a concentration of 6 nM was used for ligands in all analyses.

Quantification of the ch Afferent Terminal Distribution in the Embryonic CNS

To quantify ch afferent distribution within the embryonic CNS, stage 16.5 embryos were stained with 1D4 (for reference coordinates) and anti-GFP to visualize ch terminals expressing *UAS:syt-GFP* under the *iav-GAL4* driver. High-resolution Z stack pictures were taken using a Zeiss LSM 510 confocal microscope from a dorsal view to generate a series of optical cross-sections. Only hemisegments A2–A4 were scored for quantification (from 4 embryos/genotype for a total of 24 hemisegments/genotype; ~60.5 μm optical sections/hemisegment for a total of ~1500 sections/genotype). We avoided the region ~3 μm to either side of the ch afferent entry point into the VNC to eliminate excessive background signals from the entering ch nerve bundles and their initial branching within the CNS. At each anterior-posterior position, we used the plot profile function from NIH ImageJ software (Rasband WS, ImageJ, U.S. National Institutes of Health, Bethesda, MD; http://rsb.info.nih.gov/ij/) to determine both 1D4 and anti-GFP fluorescent signal distributions along the medial-to-lateral axis in the cross-section. For each optical section, the peak position of the 1D4-m tract signal was used as a reference point (lateral position defined as = 0 μm). Then, the lateral GFP signal distributions from all optical cross-sections were averaged to generate a normalized distribution for further analysis. Peak position of the normalized GFP distribution was defined as the lateral position of the highest GFP value in relation to the 1D4-m peak; peak width was measured at half peak height in the plotted distribution curve.

Behavioral Tests

Drosophila stocks were constructed using balancers with Tubby or GFP markers to allow selection of live larvae with desired genotypes. The *Sema-2b*^{C4} mutant was prepared in three genetic backgrounds: an isogenic line in *w1118* background; an isogenic line with the wild-type *white*$^{+}$ gene on the X chromosome in the same *w1118* background (*W*$^{+}$*/w1118*); and an isogenic line through 10 backcrosses to Canton-S line. In all three genetic backgrounds we observed similar behavioral deficits in vibration responses in mutant larvae as compared to the wild-type. We used the same *W*$^{+}$*/w1118* genetic background for all stocks analyzed in our behavioral paradigms. For vibration response tests, third instar larvae (before the wandering stage) were placed on a flat agar plate surface that permits free movement. Using the MWT and Choreography software (http://sourceforge.net) (Swierczek N., Giles A., Rankin C. and Kerr R., unpublished data), behavior of the entire larval population on the dish was tracked and analyzed. Vibration stimuli were delivered automatically. A dish with larvae was placed directly above a speaker and eight short (1 s) pulses and a longer (30 s) pulse of 1000 Hz, 1V vibration stimuli were applied at close range. The larval head turning response ("kink") was measured in Choreography, the analysis software that accompanies the MWT, using the absolute angle between the head (20% of skeleton) and the main body axis (remaining 80% of skeleton). This kink angle was quantified and compared between wild-type and mutant larvae to evaluate startle responses on vibration stimulation.

SUPPLEMENTAL INFORMATION

Supplemental Information includes seven figures and two movies and can be found with this article online at doi:10.1016/j.neuron.2011.02.050.

ACKNOWLEDGMENTS

We are very grateful to K. Venken and H. Bellen for expert support with BAC transgenic techniques, B. Dickson for the *Sema2b-τMyc* marker line and *Sema-2b* cDNA construct, C. Montell for the *iav-GAL4* stock, B. McCabe for the fourth chromosome *GFP* marker, M. Pucak and the NINDS Multi-photon Core Facility at JHMI (MH084020) for confocal imaging, and D. McClellan for her helpful comments on the manuscript. We also thank J. Cho for mapping the *UAS:PlexB*^{EcTM} stock, C. Nacopoulos for assistance with fly genetics, and members of the Kolodkin, Luo, and Zlatic laboratories for their helpful discussions throughout the course of this project. We are grateful to N. Swierczek for writing the MWT software, D. Hoffmann for building the behavioral rigs and D. Olbris, R. Svirskas, and E. Trautman for their help with behavior data analysis. We also thank the Bloomington Stock Center and the Drosophila Genome Research Center for fly stocks. This work was supported by NIH R01 NS35165 to A.L.K., R01 DC005982 to L.L., and by Janelia Farm HHMI funding to M.Z. and R.K.. R.K. and M.Z. are Fellows at Janelia Farm Howard Hughes Medical Institute; A.L.K. and L.L. are Investigators of the Howard Hughes Medical Institute.

Accepted: February 9, 2011
Published: April 27, 2011

REFERENCES

Ayoob, J.C., Terman, J.R., and Kolodkin, A.L. (2006). Drosophila Plexin B is a Sema-2a receptor required for axon guidance. Development *133*, 2125–2135.

Bastiani, M.J., Harrelson, A.L., Snow, P.M., and Goodman, C.S. (1987). Expression of fasciclin I and II glycoproteins on subsets of axon pathways during neuronal development in the grasshopper. Cell *48*, 745–755.

Bate, M., and Broadie, K. (1995). Wiring by fly: the neuromuscular system of the Drosophila embryo. Neuron *15*, 513–525.

Bates, K.E., and Whitington, P.M. (2007). Semaphorin 2a secreted by oenocytes signals through plexin B and plexin A to guide sensory axons in the Drosophila embryo. Dev. Biol. *302*, 522–535.

Bellon, A., Luchino, J., Haigh, K., Rougon, G., Haigh, J., Chauvet, S., and Mann, F. (2010). VEGFR2 (KDR/Flk1) signaling mediates axon growth in response to semaphorin 3E in the developing brain. Neuron *66*, 205–219.

Caldwell, J.C., Miller, M.M., Wing, S., Soll, D.R., and Eberl, D.F. (2003). Dynamic analysis of larval locomotion in Drosophila chordotonal organ mutants. Proc. Natl. Acad. Sci. USA *100*, 16053–16058.

Carrillo, R.A., Olsen, D.P., Yoon, K.S., and Keshishian, H. (2010). Presynaptic activity and CaMKII modulate retrograde semaphorin signaling and synaptic refinement. Neuron *68*, 32–44.

Dickson, B.J., and Zou, Y. (2010). Navigating intermediate targets: the nervous system midline. Cold Spring Harb. Perspect. Biol. *2*, a002055.

Eberl, D.F. (1999). Feeling the vibes: chordotonal mechanisms in insect hearing. Curr. Opin. Neurobiol. *9*, 389–393.

Evans, T.A., and Bashaw, G.J. (2010). Functional diversity of Robo receptor immunoglobulin domains promotes distinct axon guidance decisions. Curr. Biol. *20*, 567–572.

Farmer, W.T., Altick, A.L., Nural, H.F., Dugan, J.P., Kidd, T., Charron, F., and Mastick, G.S. (2008). Pioneer longitudinal axons navigate using floor plate and Slit/Robo signals. Development *135*, 3643–3653.

Fox, A.N., and Zinn, K. (2005). The heparan sulfate proteoglycan syndecan is an in vivo ligand for the Drosophila LAR receptor tyrosine phosphatase. Curr. Biol. *15*, 1701–1711.

Goodman, C.S., Bastiani, M.J., Doe, C.Q., du Lac, S., Helfand, S.L., Kuwada, J.Y., and Thomas, J.B. (1984). Cell recognition during neuronal development. Science *225*, 1271–1279.

Grenningloh, G., Rehm, E.J., and Goodman, C.S. (1991). Genetic analysis of growth cone guidance in Drosophila: fasciclin II functions as a neuronal recognition molecule. Cell *67*, 45–57.

Harrelson, A.L., and Goodman, C.S. (1988). Growth cone guidance in insects: fasciclin II is a member of the immunoglobulin superfamily. Science *242*, 700–708.

Hidalgo, A., and Booth, G.E. (2000). Glia dictate pioneer axon trajectories in the Drosophila embryonic CNS. Development *127*, 393–402.

Hidalgo, A., and Brand, A.H. (1997). Targeted neuronal ablation: the role of pioneer neurons in guidance and fasciculation in the CNS of Drosophila. Development *124*, 3253–3262.

Hiramoto, M., and Hiromi, Y. (2006). ROBO directs axon crossing of segmental boundaries by suppressing responsiveness to relocalized Netrin. Nat. Neurosci. *9*, 58–66.

Hiramoto, M., Hiromi, Y., Giniger, E., and Hotta, Y. (2000). The Drosophila Netrin receptor Frazzled guides axons by controlling Netrin distribution. Nature *406*, 886–889.

Hu, H., Marton, T.F., and Goodman, C.S. (2001). Plexin B mediates axon guidance in Drosophila by simultaneously inhibiting active Rac and enhancing RhoA signaling. Neuron *32*, 39–51.

Hulsmeier, J., Pielage, J., Rickert, C., Technau, G.M., Klambt, C., and Stork, T. (2007). Distinct functions of alpha-Spectrin and beta-Spectrin during axonal pathfinding. Development *134*, 713–722.

Jarman, A.P., Grau, Y., Jan, L.Y., and Jan, Y.N. (1993). atonal is a proneural gene that directs chordotonal organ formation in the Drosophila peripheral nervous system. Cell *73*, 1307–1321.

Khare, N., Fascetti, N., DaRocha, S., Chiquet-Ehrismann, R., and Baumgartner, S. (2000). Expression patterns of two new members of the Semaphorin family in Drosophila suggest early functions during embryogenesis. Mech. Dev. *91*, 393–397.

Kuwada, J.Y. (1986). Cell recognition by neuronal growth cones in a simple vertebrate embryo. Science *233*, 740–746.

Kwon, Y., Shen, W.L., Shim, H.S., and Montell, C. (2010). Fine thermotactic discrimination between the optimal and slightly cooler temperatures via a TRPV channel in chordotonal neurons. J. Neurosci. *30*, 10465–10471.

Landgraf, M., Sanchez-Soriano, N., Technau, G.M., Urban, J., and Prokop, A. (2003). Charting the Drosophila neuropile: a strategy for the standardised characterisation of genetically amenable neurites. Dev. Biol. *260*, 207–225.

Lee, T., and Luo, L. (1999). Mosaic analysis with a repressible cell marker for studies of gene function in neuronal morphogenesis. Neuron *22*, 451–461.

Lin, D.M., Fetter, R.D., Kopczynski, C., Grenningloh, G., and Goodman, C.S. (1994). Genetic analysis of Fasciclin II in Drosophila: defasciculation, refasciculation, and altered fasciculation. Neuron *13*, 1055–1069.

Long, H., Sabatier, C., Ma, L., Plump, A., Yuan, W., Ornitz, D.M., Tamada, A., Murakami, F., Goodman, C.S., and Tessier-Lavigne, M. (2004). Conserved roles for Slit and Robo proteins in midline commissural axon guidance. Neuron *42*, 213–223.

Lopez-Bendito, G., Flames, N., Ma, L., Fouquet, C., Di Meglio, T., Chedotal, A., Tessier-Lavigne, M., and Marin, O. (2007). Robo1 and Robo2 cooperate to control the guidance of major axonal tracts in the mammalian forebrain. J. Neurosci. *27*, 3395–3407.

Mann, F., Chauvet, S., and Rougon, G. (2007). Semaphorins in development and adult brain: Implication for neurological diseases. Prog. Neurobiol. *82*, 57–79.

Mastick, G.S., Farmer, W.T., Altick, A.L., Nural, H.F., Dugan, J.P., Kidd, T., and Charron, F. (2010). Longitudinal axons are guided by Slit/Robo signals from the floor plate. Cell Adh. Migr. *4*, 337–341.

Matsuoka, R.L., Nguyen-Ba-Charvet, K.T., Parray, A., Badea, T.C., Chedotal, A., and Kolodkin, A.L. (2011). Transmembrane semaphorin signalling controls laminar stratification in the mammalian retina. Nature *470*, 259–263.

Matthes, D.J., Sink, H., Kolodkin, A.L., and Goodman, C.S. (1995). Semaphorin II can function as a selective inhibitor of specific synaptic arborizations. Cell *81*, 631–639.

Merritt, D.J., and Whitington, P.M. (1995). Central projections of sensory neurons in the Drosophila embryo correlate with sensory modality, soma position, and proneural gene function. J. Neurosci. *15*, 1755–1767.

Nose, A., Mahajan, V.B., and Goodman, C.S. (1992). Connectin: a homophilic cell adhesion molecule expressed on a subset of muscles and the motoneurons that innervate them in Drosophila. Cell *70*, 553–567.

Parks, A.L., Cook, K.R., Belvin, M., Dompe, N.A., Fawcett, R., Huppert, K., Tan, L.R., Winter, C.G., Bogart, K.P., Deal, J.E., et al. (2004). Systematic generation of high-resolution deletion coverage of the Drosophila melanogaster genome. Nat. Genet. *36*, 288–292.

Pecho-Vrieseling, E., Sigrist, M., Yoshida, Y., Jessell, T.M., and Arber, S. (2009). Specificity of sensory-motor connections encoded by Sema3e-Plxnd1 recognition. Nature *459*, 842–846.

Rajagopalan, S., Vivancos, V., Nicolas, E., and Dickson, B.J. (2000). Selecting a longitudinal pathway: Robo receptors specify the lateral position of axons in the Drosophila CNS. Cell *103*, 1033–1045.

Raper, J., and Mason, C. (2010). Cellular strategies of axonal pathfinding. Cold Spring Harb. Perspect. Biol. *2*, a001933.

Ritzenthaler, S., Suzuki, E., and Chiba, A. (2000). Postsynaptic filopodia in muscle cells interact with innervating motoneuron axons. Nat. Neurosci. *3*, 1012–1017.

Sanes, J.R., and Yamagata, M. (2009). Many paths to synaptic specificity. Annu. Rev. Cell Dev. Biol. *25*, 161–195.

Simpson, J.H., Bland, K.S., Fetter, R.D., and Goodman, C.S. (2000). Short-range and long-range guidance by Slit and its Robo receptors: a combinatorial code of Robo receptors controls lateral position. Cell *103*, 1019–1032.

Spitzweck, B., Brankatschk, M., and Dickson, B.J. (2010). Distinct protein domains and expression patterns confer divergent axon guidance functions for Drosophila Robo receptors. Cell *140*, 409–420.

Swan, L.E., Wichmann, C., Prange, U., Schmid, A., Schmidt, M., Schwarz, T., Ponimaskin, E., Madeo, F., Vorbruggen, G., and Sigrist, S.J. (2004). A glutamate receptor-interacting protein homolog organizes muscle guidance in Drosophila. Genes Dev. *18*, 223–237.

Tessier-Lavigne, M., and Goodman, C.S. (1996). The molecular biology of axon guidance. Science *274*, 1123–1133.

Toyofuku, T., Yoshida, J., Sugimoto, T., Yamamoto, M., Makino, N., Takamatsu, H., Takegahara, N., Suto, F., Hori, M., Fujisawa, H., et al. (2008). Repulsive and attractive semaphorins cooperate to direct the navigation of cardiac neural crest cells. Dev. Biol. *321*, 251–262.

Vactor, D.V., Sink, H., Fambrough, D., Tsoo, R., and Goodman, C.S. (1993). Genes that control neuromuscular specificity in Drosophila. Cell *73*, 1137–1153.

Venken, K.J., He, Y., Hoskins, R.A., and Bellen, H.J. (2006). P[acman]: a BAC transgenic platform for targeted insertion of large DNA fragments in D. melanogaster. Science *314*, 1747–1751.

Winberg, M.L., Mitchell, K.J., and Goodman, C.S. (1998a). Genetic analysis of the mechanisms controlling target selection: complementary and combinatorial functions of netrins, semaphorins, and IgCAMs. Cell *93*, 581–591.

Winberg, M.L., Noordermeer, J.N., Tamagnone, L., Comoglio, P.M., Spriggs, M.K., Tessier-Lavigne, M., and Goodman, C.S. (1998b). Plexin A is a neuronal semaphorin receptor that controls axon guidance. Cell *95*, 903–916.

Winberg, M.L., Tamagnone, L., Bai, J., Comoglio, P.M., Montell, D., and Goodman, C.S. (2001). The transmembrane protein Off-track associates

with Plexins and functions downstream of Semaphorin signaling during axon guidance. Neuron *32*, 53–62.

Wolman, M.A., Regnery, A.M., Becker, T., Becker, C.G., and Halloran, M.C. (2007). Semaphorin3D regulates axon axon interactions by modulating levels of L1 cell adhesion molecule. J. Neurosci. *27*, 9653–9663.

Wolman, M.A., Sittaramane, V.K., Essner, J.J., Yost, H.J., Chandrasekhar, A., and Halloran, M.C. (2008). Transient axonal glycoprotein-1 (TAG-1) and laminin-alpha1 regulate dynamic growth cone behaviors and initial axon direction in vivo. Neural Dev. *3*, 6.

Yao, K.M., and White, K. (1994). Neural specificity of elav expression: defining a Drosophila promoter for directing expression to the nervous system. J. Neurochem. *63*, 41–51.

Yoshida, Y., Han, B., Mendelsohn, M., and Jessell, T.M. (2006). PlexinA1 signaling directs the segregation of proprioceptive sensory axons in the developing spinal cord. Neuron *52*, 775–788.

Yu, H.H., Araj, H.H., Ralls, S.A., and Kolodkin, A.L. (1998). The transmembrane Semaphorin Sema I is required in Drosophila for embryonic motor and CNS axon guidance. Neuron *20*, 207–220.

Zlatic, M., Landgraf, M., and Bate, M. (2003). Genetic specification of axonal arbors: atonal regulates robo3 to position terminal branches in the Drosophila nervous system. Neuron *37*, 41–51.

Zlatic, M., Li, F., Strigini, M., Grueber, W., and Bate, M. (2009). Positional cues in the Drosophila nerve cord: semaphorins pattern the dorso-ventral axis. PLoS Biol. *7*, e1000135. 10.1371/journal.pbio.1000135.

Neuron, Volume *70*

Supplemental Information

A Combinatorial Semaphorin Code Instructs the Initial Steps of Sensory Circuit Assembly in the *Drosophila* CNS

Zhuhao Wu, Lora B. Sweeney, Joseph C. Ayoob, Kayam Chak, Benjamin J. Andreone, Tomoko Ohyama, Rex Kerr, Liqun Luo, Marta Zlatic, and Alex L. Kolodkin

Inventory of Supplemental Information

Movie S1, related to Figure 7: Startle response of a single Wild-type *Drosophila* larvae to vibration.

Movie S2, related to Figure 7: Computer-generated tracing of a group of larvae before and after a vibration stimulus.

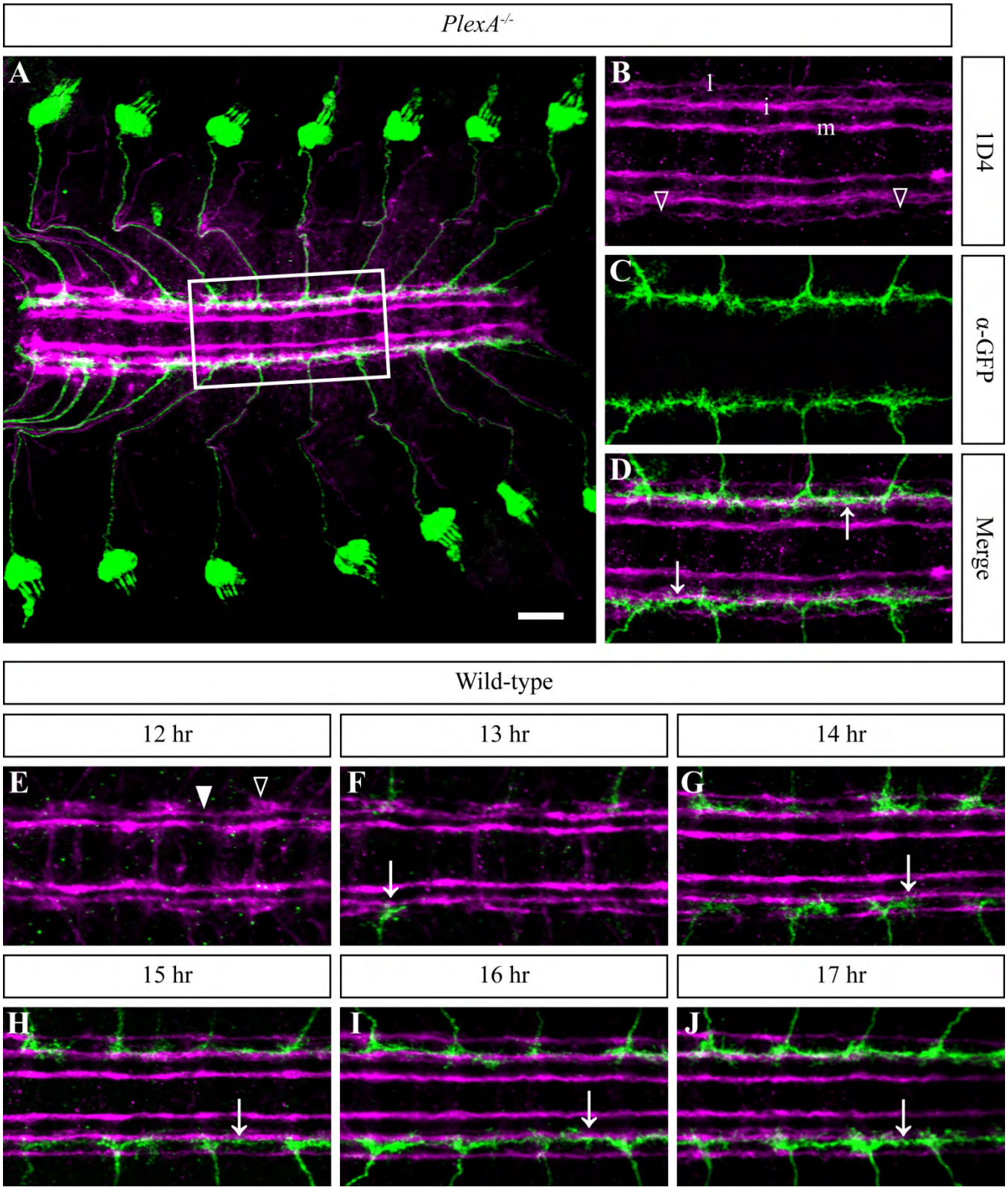
PlexA-/-
A
B
l
i
m
1D4
C
α-GFP
D
Merge
Wild-type
12 hr
13 hr
14 hr
E
F
G
15 hr
16 hr
17 hr
H
I
J

Figure S1, related to Figure 1. Ch sensory axons navigate along the intermediate 1D4 tract in the CNS.

(A–D) Dorsal views of embryos stained with 1D4 (magenta) and anti-GFP (green). (A) In *PlexA*$^{-/-}$ mutant embryos, ch axons navigate into the CNS along the ISN pathway. (B) *PlexA*$^{-/-}$ mutant embryos show distinct CNS defects; the lateral 1D4 tract is often thin and discontinuous (empty arrowheads), but the intermediate 1D4 tract appears normal. (C, D) Ch axons show normal terminal bifurcations along the intermediate 1D4 tract in *PlexA*$^{-/-}$ mutants.

(E–J) The developmental progression of ch innervation within the CNS from 12 hr after-egg-laying (AEL) to 17 hr AEL in the wild-type embryos. (E) At 12 hr AEL, the intermediate 1D4 tract is well established (arrowhead), while the lateral 1D4 tract is just starting to form (empty arrowhead). At this stage, ch neuron axons are extending along the ISN pathway toward the CNS, however few have reached CNS longitudinal pathways. (F) Some ch axons start to appear within the CNS at 13 hr AEL (arrow). They stop growing medially after reaching the intermediate CNS region and then bifurcate along the surface of the intermediate 1D4 tract. (G) At 14 hr AEL, most ch axons have bifurcated within the CNS in each segment, extending branches both anteriorly and posteriorly. (H) At 15 hr AEL, ch axons have extended branches along the intermediate 1D4 tract and overlap with branches extending from the adjacent segments. (I and J) At 16 hr AEL and thereafter, most ch axon branches have joined with adjacent segments, forming a continuous longitudinal innervation tract.

Scale bar in A: 20μm for A; 10μm for B–J.

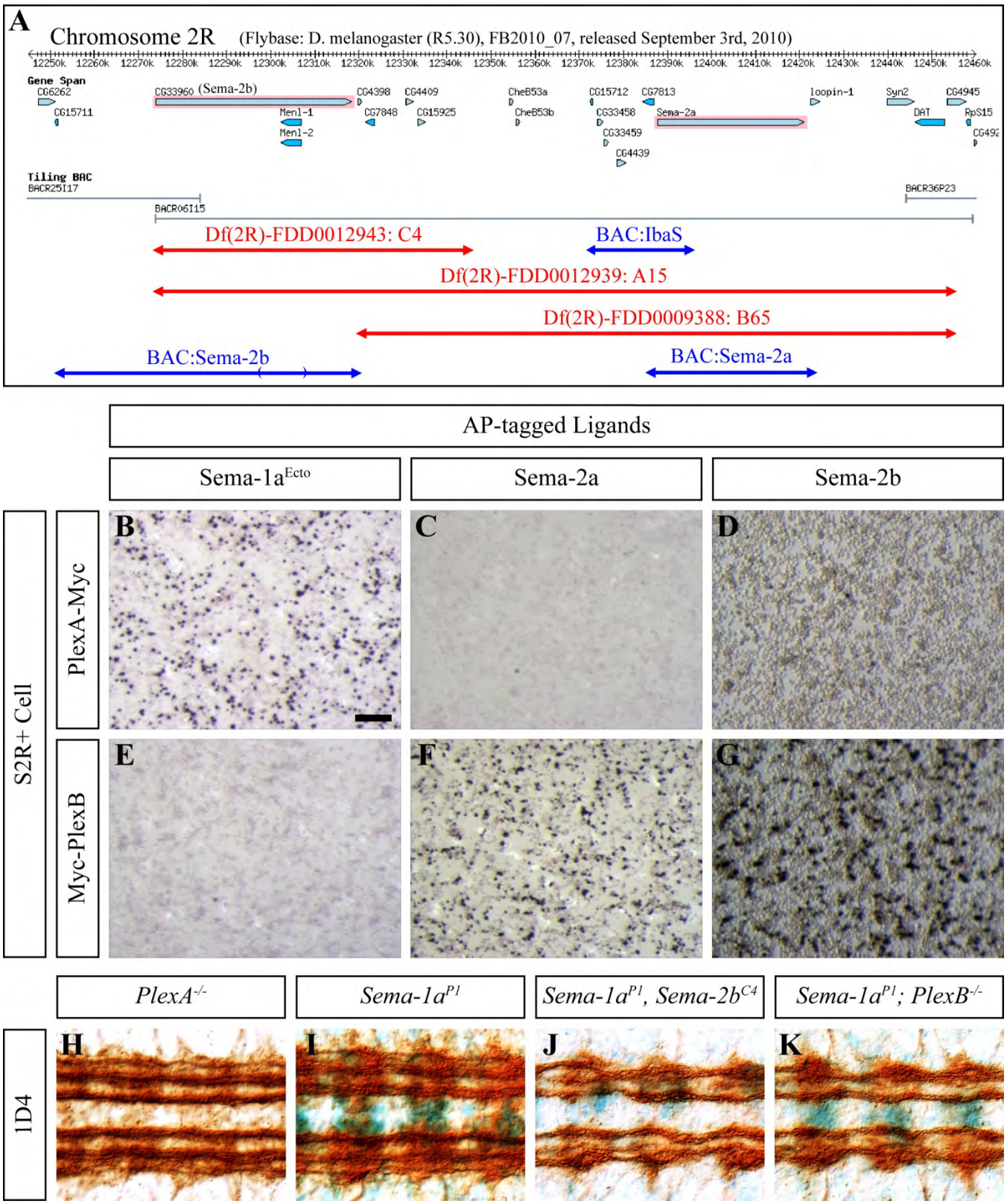
A
Chromosome 2R (Flybase: D. melanogaster (R5.30), FB2010_07, released September 3rd, 2010)
12250k 12260k 12270k 12280k 12290k 12300k 12310k 12320k 12330k 12340k 12350k 12360k 12370k 12380k 12390k 12400k 12410k 12420k 12430k 12440k 12450k 12460k
Gene Span
CG6262
CG15711
CG33960 (Sema-2b)
Men1-1
Men1-2
CG4398
CG7848
CG4409
CG15925
CheB53a
CheB53b
CG15712
CG7813
CG33458
CG33459
CG4439
Sema-2a
loopin-1
Syn2
DAT
CG4945
RpS15
Tiling BAC
BACR25I17
BACR06I15
BACR36P23
Df(2R)-FDD0012943: C4
BAC:IbaS
Df(2R)-FDD0012939: A15
Df(2R)-FDD0009388: B65
BAC:Sema-2b
BAC:Sema-2a
AP-tagged Ligands
Sema-1a^Ecto
Sema-2a
Sema-2b
S2R+ Cell
PlexA-Myc
Myc-PlexB
B
C
D
E
F
G
PlexA-/-
Sema-1aP1
Sema-1aP1, Sema-2bC4
Sema-1aP1; PlexB-/-
1D4
H
I
J
K

Figure S2, related to Figure 2. Generation of *Sema-2b* and *Sema-2a* mutants, binding specificities of these secreted semaphorin ligands to plexin receptors, and distinct CNS functions compared to transmembrane *Sema-1a*.

(A) Genomic deletions and transgenes corresponding to the local genomic region covering both the *Sema-2a* and *Sema-2b* genes. The FRT-containing P elements *d00549* and *f02115* were used to generate genomic deletions covering *Sema-2a* (*FDD-000938: Sema2a*^{B65}). The genomic region between *Sema-2a* and *Sema-2b* contains a haplo-insufficient element which we mapped by complementation to the region covered by the genomic transgene *BAC:IbaS*. The fly stock containing both the *BAC:IbaS* transgene and the *FDD-000938* deficiency was kept as a stable stock to make the *Sema-2a*^{B65} null mutant. P elements *d00791* and *f05499* were used to make a deficiency (*FDD-0012943: C4*) that serves as a *Sema-2b* null mutant (*Sema-2b*^{C4}). P elements d00791 and f02115 were used to remove both *Sema-2a* and *Sema-2b*, and the deletion (*FDD-0012939: A15*) was combined with the *BAC:IbaS* transgene to make a stable stock that serves as the *Sema-2a, Sema-2b* double null mutant (*Sema-2ab*^{A15}). *BAC:IbaS* was subcloned from the *BACR06I15* BAC construct in order to cover genes from *CG15712* to *CG7813*. The *BAC:Sema-2a* transgene was subcloned from the *BACR06I15* BAC construct so as to cover only the *Sema-2a* genomic region. The *BAC:Sema-2b* transgene was assembled using *BACR25I17* and *BACR06I15* BAC constructs in order to cover the whole *Sema-2b* genomic region; subsequently, the *Menl-1&2* genes were removed to ensure coverage of only the *Sema-2b* gene.

(B–G) Cultured S2R+ cells transfected with expression constructs for either PlexA (B–D) or PlexB (E–G) and then incubated with a soluble AP–tagged extracellular domain (EC) of Sema-1a (Sema-1a^{EC}–AP) (B and E), Sema-2a–AP (C and F), or Sema-2b–AP (D and G). (B) Sema-1a^{EC}–AP binds to the surface of S2R+ cells transfected with PlexA. (C and D) Neither Sema-2a–AP nor Sema-2b–AP binds to S2R+ cells transfected with PlexA. (E) Sema-1a^{EC}–AP does not bind to S2R+ cells transfected with PlexB. (F

and G) Both Sema-2a–AP and Sema-2b–AP bind to S2R+ cells transfected with PlexB.

(H–K) Late stage 16 embryos were stained with 1D4 MAb to reveal the formation of CNS longitudinal tracts. In *PlexA*$^{-/-}$ (H) or *Sema-1a*$^{-/-}$ (I) mutants the lateral 1D4 tract is often thin and discontinuous, while the intermediate 1D4 tract appears normal. In *Sema-1a*, *Sema-2b* double null mutant embryos (J), or *Sema-1a*, *PlexB* double null mutants (K), both the lateral and the intermediate 1D4 tracts are severely disrupted. In most segments they fuse into a thick tangled bundle, demonstrating an additive effect resulting from removing *Sema-1a* and either *Sema-2b* or *PlexB*. These genetic analyses indicate that *Sema-1a/PlexA* signaling mediates CNS functions distinct from those governed by *Sema-2b/PlexB* signaling, suggesting these ligand receptor pairs do not function in the same genetic pathway.

Scale bar in B: 35μm for B–G; 10μm for H–K.

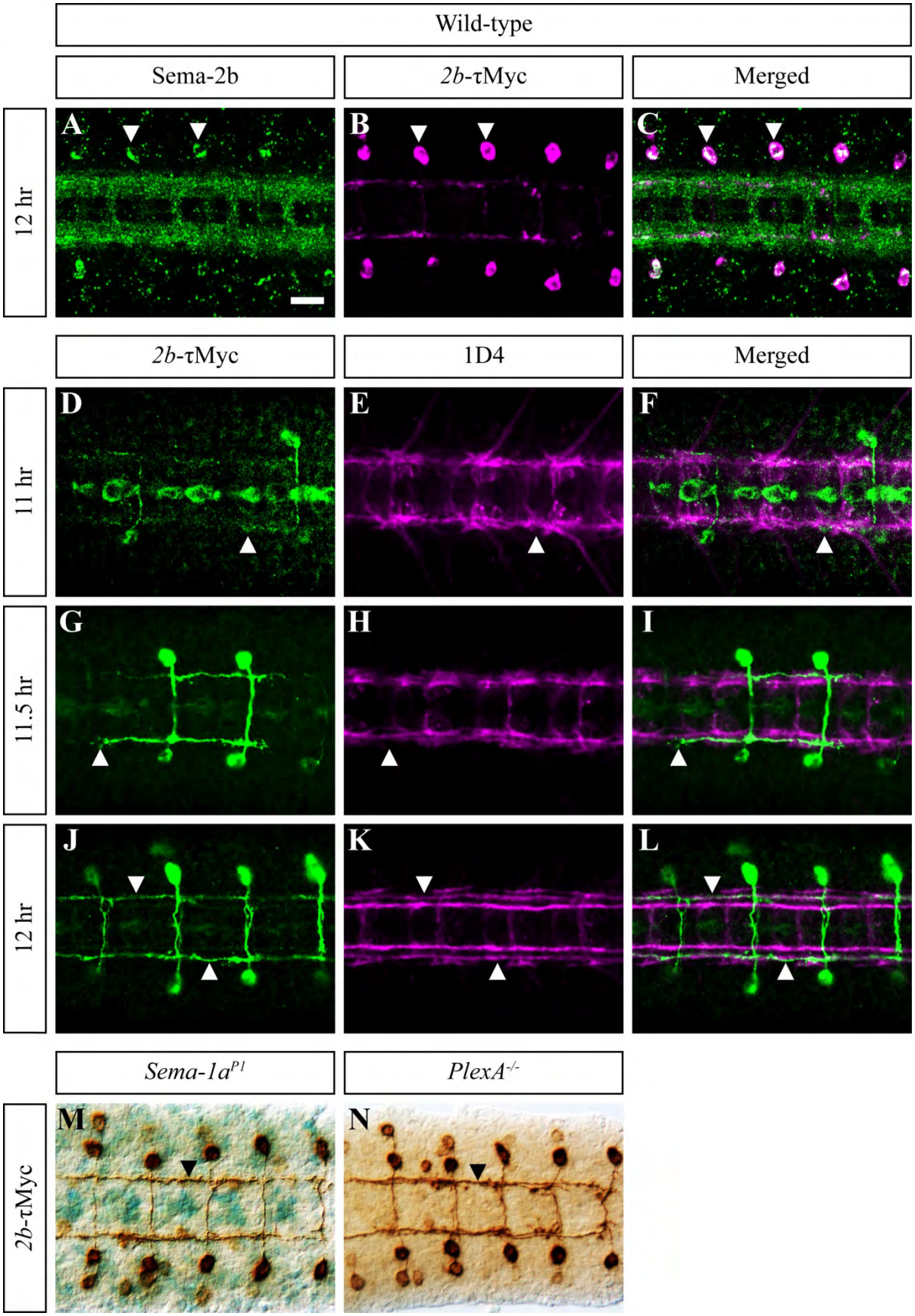
Wild-type
Sema-2b
2b-τMyc
Merged
12 hr
A
B
C
2b-τMyc
1D4
Merged
11 hr
D
E
F
11.5 hr
G
H
I
12 hr
J
K
L
Sema-1a^P1
PlexA^-/-
2b-τMyc
M
N

Figure S3, related to Figure 3. Sema-2b expression, the timing of Sema-2b^{+} connective assembly, and its independence from Sema1a/PlexA signaling.

(A–C) The *2b-τMyc* neurons express high levels of Sema-2b as revealed by anti-Sema2b immunostaining. Their cell bodies express elevated levels of Sema-2b (arrowheads).

(D–L) *2b-τMyc* longitudinal pathway formation was examined between 11 hr and 12 hr AEL. (D–F) At 11 hr AEL, some *2b-τMyc* neurons already have elaborated axons that cross the CNS midline and project anteriorly. The intermediate 1D4^{+} pathway is still part of the single loose 1D4^{+} bundle present in the CNS at this stage, and the longitudinal *2b-τMyc* axons project just lateral to the developing 1D4^{+} pathway. (G–I) At 11.5 hr AEL the *2b-τMyc* axons join each other in adjacent segments and continue growing anteriorly. The intermediate 1D4^{+} tract has started to separate from the medial 1D4^{+} tract, trailing behind the *2b-τMyc* longitudinal axons. (J–L) At 12 hr AEL the *2b-τMyc* longitudinal pathway has fully developed, and the intermediate 1D4^{+} tract is also well established.

(M and **N)** In *Sema-1a*$^{-/-}$ or *PlexA*$^{-/-}$ mutant embryos, the *2b-τMyc* pathway still forms correctly.

Scale bar in A: 10μm for A–L; 13μm for M and N.

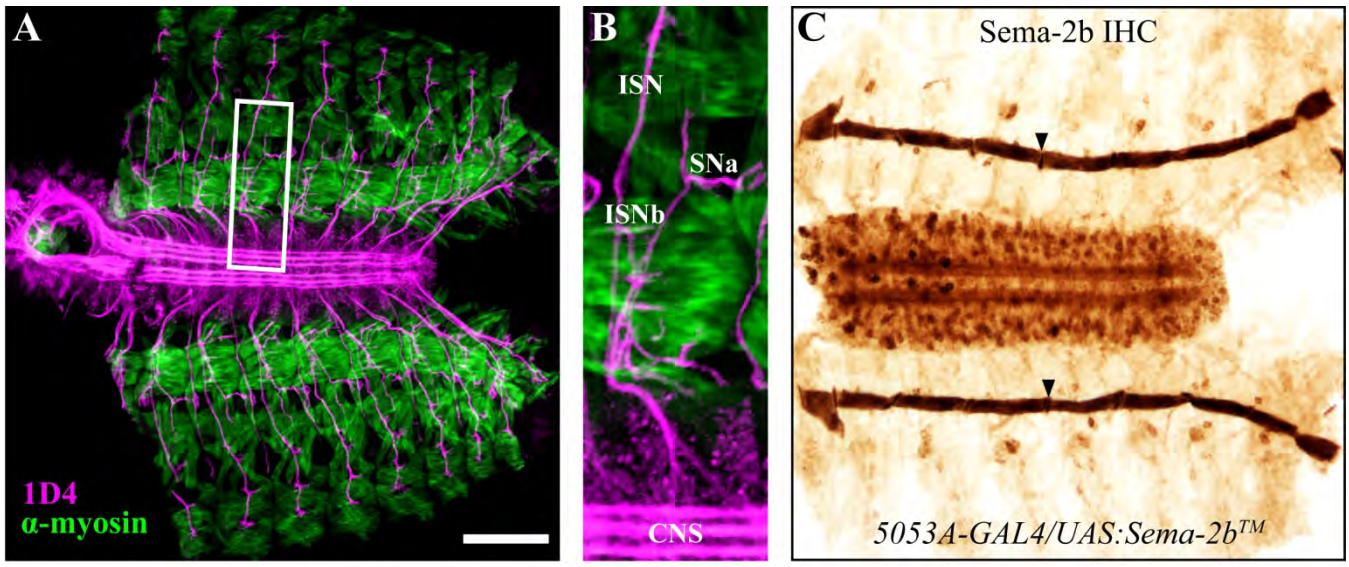

D Muscle-12 *5053A-GAL4* GOF Phenotype Quantification

Genotype	Abnormal ISNb Pathway (hemisegments)[a]	Abnormal SNa Pathway (hemisegments)[b]
Controls		
Wild-type	3.3% (n=240)	0.4% (n=237)
5053A-GAL4/+	8.9% (n=246)	1.2% (n=250)
1 Copy GOF		
UAS:Sema-2a ™/+; 5053A-GAL4/+	24.9% (n=225)	0.0% (n=240)
UAS:Sema-2b ™/+; 5053A-GAL4/+	7.9% (n=165)	5.4% (n=240)
2 Copy GOF[c]		
UAS:Sema-2a ™/UAS:Sema-2a ™; 5053A-GAL4/+	52.6% (n=95)	5% (n=100)
UAS:Sema-2b ™/UAS:Sema-2b ™; 5053A-GAL4/+	9.3% (n=86)	28.2% (n=100)

[a]ISNb phenotype: ISNb motor axons reached muscle 12 with no RP5 innervations.

[b]SNa phenotype: SNa lateral branch pathway bent to keep contact with muscle 12.

[c]Two copy UAS transgene overexpression was still drived by one copy of *5053A-GAL4* .

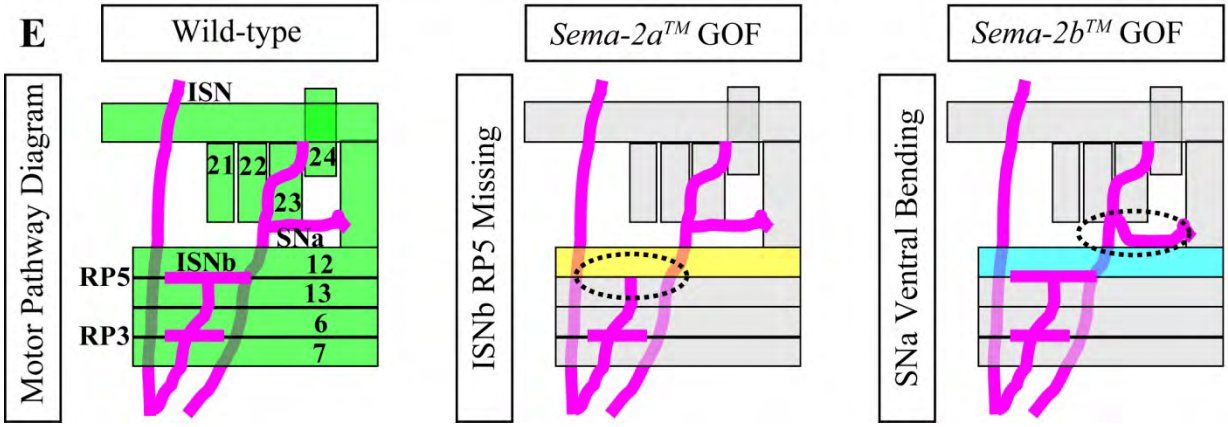

Figure S4, related to Figure 4. Quantification of motor axon defects in embryos following Sema-2a or Sema-2b overexpression in muscle 12.

(A and **B)** Filleted preparation of a late stage 16 wild-type embryo, stained with 1D4 (magenta) and anti-Myosin antibody (green), showing stereotypic CNS axonal trajectories and peripheral neural-muscular connectivity. The hemisegment region boxed in (A) is shown at higher magnification in (B) to highlight the ISNb and SNa innervation patterns.

(C) The *5053A-GAL4* driver directs *UAS:Sema-2b^{TM}* expression in muscle 12. Sema-2b staining reveals ectopically expressed membrane-tethered Sema-2b as a continuous rostral-to-caudal strip on muscle 12 within the body wall along each side of the embryo (arrowheads), and also shows endogenous Sema-2b expression in the CNS.

(D) Quantification of the motor pathway defects observed in control embryos, 1 copy GOF, and 2 copy GOF embryos expressing *Sema-2a^{TM}* or *Sema-2b^{TM}* solely in muscle 12.

(E) Diagrams summarize innervation patterns for SNa and ISNb pathways in a wild-type background, and the specific defects induced by *Sema-2a^{TM}* or *Sema-2b^{TM}* GOF in muscle 12. ISNb axons defasciculate between muscles 6 and 7 to form synaptic arborizations on these muscles, and then defasciculate between muscles 12 and 13 to form synaptic arborizations on these more dorsal muscles. When Sema-2a^{TM} is over expressed in muscle 12, ISNb RP5 innervation often fails to occur, indicative of axonal repulsion. The lateral branch from the SNa pathway usually navigates nearby muscle 12 but does not contact it. Ectopically expressed Sema-2b^{TM} from muscle 12 leads to extensive ectopic association of the SNa lateral branch with muscle-12, strongly suggesting that Sema-2b promotes axonal attraction.

Scale bar in A: 34μm for A; 10μm for B; 30μm for C.

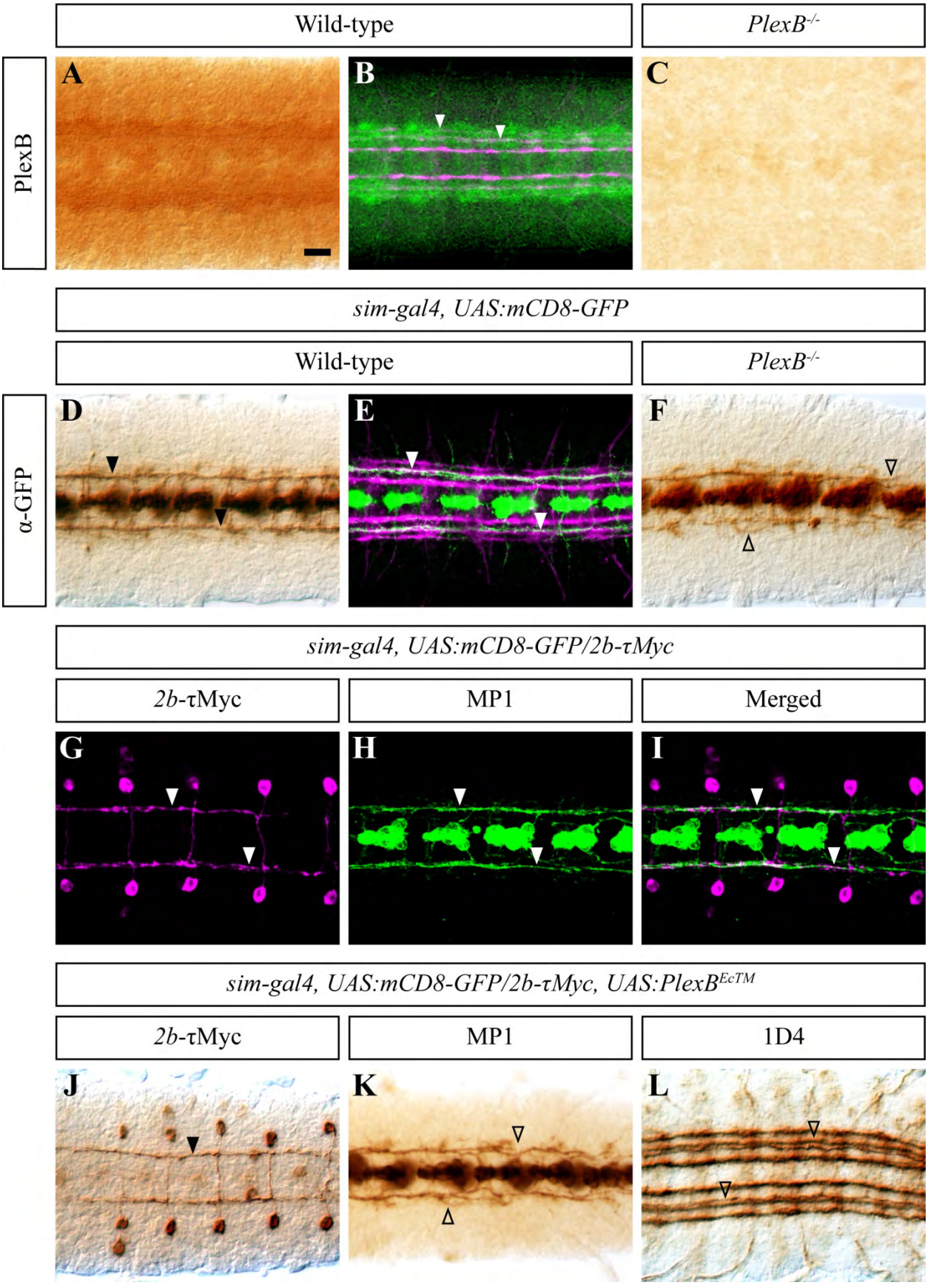
Wild-type
PlexB-/-
PlexB
A
B
C
sim-gal4, UAS:mCD8-GFP
Wild-type
PlexB-/-
α-GFP
D
E
F
sim-gal4, UAS:mCD8-GFP/2b-τMyc
2b-τMyc
MP1
Merged
G
H
I
sim-gal4, UAS:mCD8-GFP/2b-τMyc, UAS:PlexBEcTM
2b-τMyc
MP1
1D4
J
K
L

Figure S5, related to Figure 5. PlexB requirements for embryonic longitudinal pathway assembly.

(A–C) Stage-15/16 embryonic CNS stained with a rabbit polyclonal antibody directed against PlexB. The PlexB protein is widely distributed within in the CNS (A), and expression appears elevated in the intermediate-to-lateral region of the CNS longitudinal pathway (arrowheads in B). (C) PlexB expression is absent in *PlexB*$^{-/-}$ mutant embryos.

(D) MP1 neurons are labeled by the *sim-GAL4* driver, allowing observation of their axons joining to form a single longitudinal fascicle. **(E)** The MP1 longitudinal pathway is part of the intermediate 1D4^{+} tract, and during the development the MP1 pathway pioneers this 1D4 tract (Hidalgo and Brand, 1997). **(F)** In *PlexB*$^{-/-}$ mutants, the MP1 pathway is often disorganized, defasciculated, and discontinuous.

(G–I) The MP1 longitudinal pathway shares the same lateral position with the *2b-τMyc* longitudinal pathway, as visualized utilizing the *sim-GAL4*–drived GFP expression and *2b*-τMyc marker. **(J–L)** A dominant-negative form of PlexB over-expressed in MP1 neurons using the *sim-GAL4* driver does not disrupt formation of the *2b-τMyc* pathway (J), however, the MP1 pathway (K) and the intermediate 1D4^{+} pathway (L) are both often defasciculated.

Scale bar in A: 10μm for A–L.

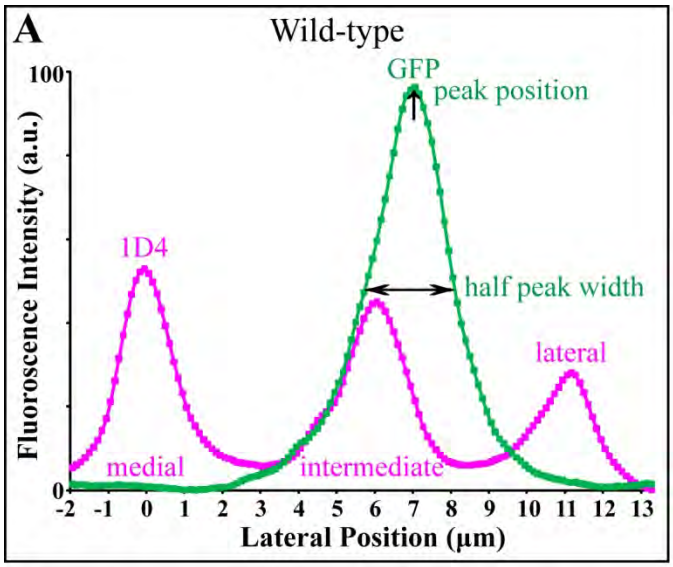

B Distribution of Ch Afferent Terminals

Genotype	iav-GFP peak (µm)		n (cross-sections)
	Position	Width	
Wild-type	7.1	2.3	*1463*
Sema-2a^{B65}	6.9	2.6	*1405*
Sema-2b^{C4}	9.0	3.3	*1519*
Sema-2ab^{A15}	7.2	5.1	*1565*
PlexB$^{-/-}$	7.1	5.0	*1721*

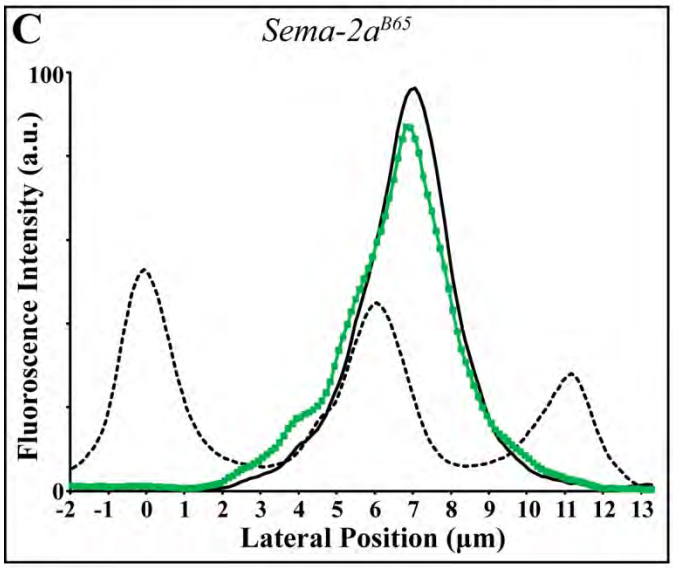

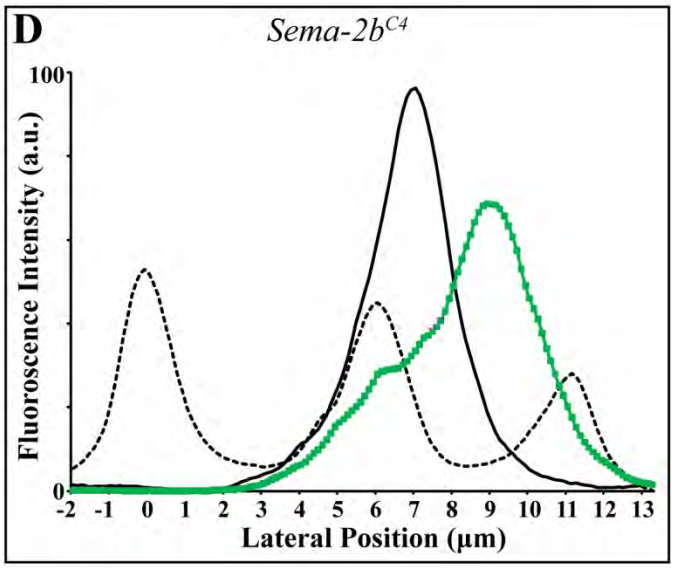

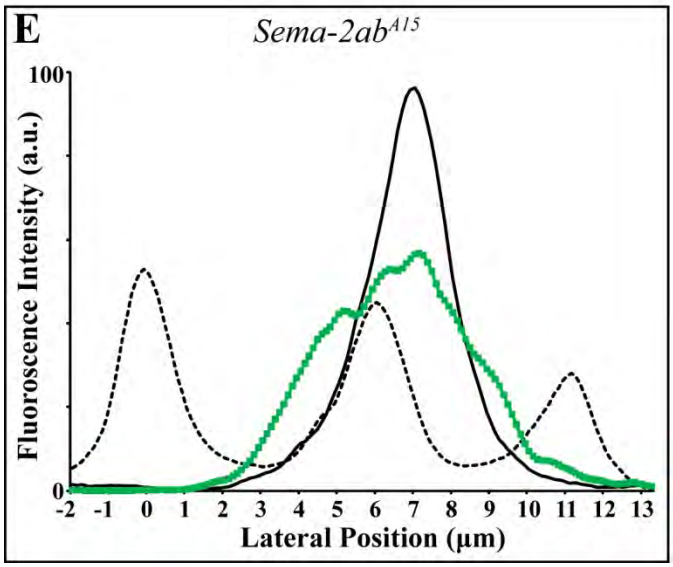

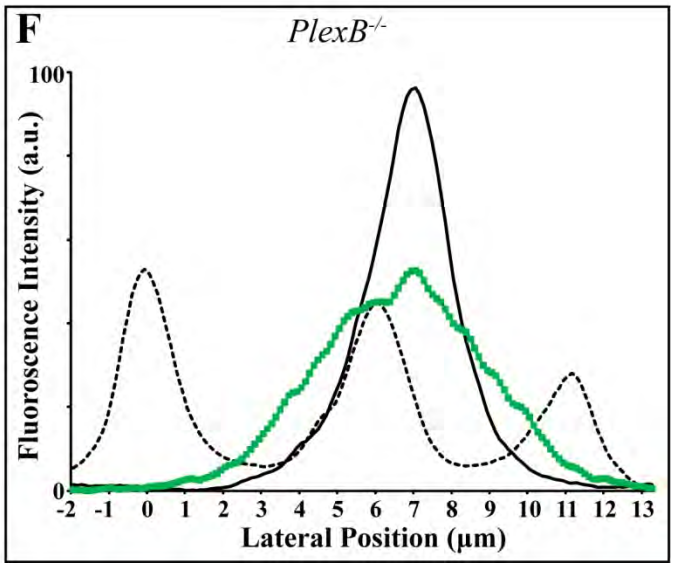

Figure S6, related to Figure 6. Additional quantification of ch afferent targeting in wild-type and *Sema-2a, Sema-2b,* and *PlexB* mutants.

(A) Ch afferent targeting within the CNS was analyzed by determining the medial-to-lateral distribution of *iav*-GFP signal (green line) compared with the 1D4 (magenta line) distribution within CNS segments as indicated in the legend to Figure 6, and also in the Experimental Procedures. The medial $1D4^{+}$ peak was used as reference point (lateral position = 0μm) for each cross-section, then the GFP signal distributions from all optical cross-sections were averaged to generate the normalized distribution for further analysis. Peak position of the normalized GFP distribution was defined as the lateral position of the highest GFP value to the medial 1D4 peak; peak width is measured at half peak height. **(B)** Summary of *iav*-GFP peak position and width in different genetic backgrounds. **(C–F)** Distributions of *iav*-GFP (green line) in $Sema\text{-}2a^{B65}$, $Sema\text{-}2b^{C4}$, $Sema\text{-}2a2b^{A15}$, and $PlexB^{-/-}$ mutant embryos are compared in each graph to wild-type *iav*-GFP (black line) and 1D4 (dashed black line) distributions.

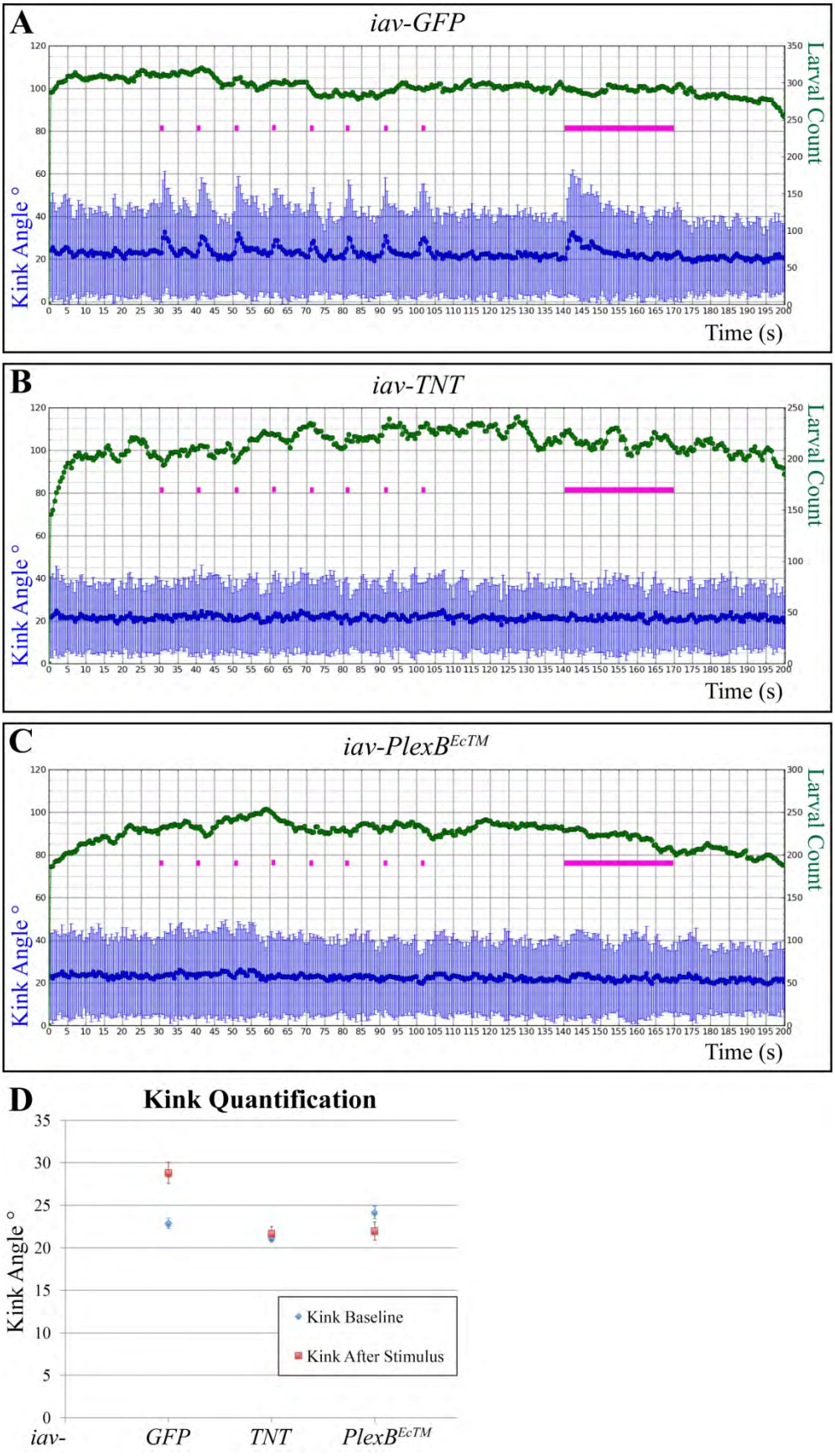
A
iav-GFP
Kink Angle °
Larval Count
Time (s)
B
iav-TNT
Kink Angle °
Larval Count
Time (s)
C
iav-PlexB^EcTM
Kink Angle °
Larval Count
Time (s)
D
Kink Quantification
Kink Angle °
Kink Baseline
Kink After Stimulus
iav-
GFP
TNT
PlexB^EcTM

Figure S7, related to Figure 7. PlexB-mediated signaling is required in ch neurons for normal larval reaction to vibration.

(A–C) Graphs show mean head turning angle (in degrees) as a function of time for positive control *iav-GAL4,UAS-CD8GFP* (*iav-GFP*), negative control *iav-GAL4,UAS-TNT* (*iav-TNT*), and *iav-GAL4,UAS-PlexB^{EcTM}* (*iav-PlexB^{EcTM}*) larvae. Larval samples of each genotype were tracked for 200 sec. As described in the legend to Figure 7 and in the Experimental Procedures, eight short (1 sec) pulses of 1000 Hz vibration were presented to the larvae at 30, 40, 50, 60, 70, 80, 90 and 100 sec. A longer (30 sec) of 1000 Hz vibration stimulus was presented from 140-170 sec. Blue dots show mean absolute angles for the population of larvae tracked in each 0.5 sec time interval. Blue error bars show standard deviation from the mean angle in each 0.5 sec time interval. Green dots show the number of larvae tracked by the software within each 0.5 sec interval. (A) Negative control *iav-GFP* larvae react to vibration by turning their heads and stopping. Note the marked increases in mean angle following each vibration stimulus. (B) Positive control *iav-TNT* larvae, in which ch neurons are inactivated, do not turn in response to vibration. Note the absence of marked increases in mean angle following each vibration stimulus. (C) Similar to *iav-TNT* larvae, *iav-PlexB^{EcTM}* larvae do not turn in response to vibration.

(D) Quantification of head turning in response to vibration of *iav-GFP*, *iav-TNT*, and *iav-PlexB^{EcTM}* larvae. Blue marks show mean angle between head and main body axis of larvae in the pre-stimulus time interval (15-30 sec) as the baseline values. Blue error bars show standard errors of the mean relative baseline values during this 15 sec time interval prior to stimulus presentation. Red marks show mean angle of larvae in a 1 sec interval during the presentation of vibration stimulus (141-142 sec). Red error bars show standard errors of the mean in the 1 sec interval during the presentation of the vibration stimulus. The baseline values (before stimuli) were similar in larvae of all three genotypes. However, only positive control (*iav-GFP*) larvae exhibit significantly increased turning during vibration

relative to the baseline ($p<0.001$; student t-test). The negative control (*iav-TNT*) and *iav-PlexB*^{EcTM} larvae do not show significantly increased turning in response to vibration ($p<0.001$, student t-test). Therefore, the mean angle values during vibration observed in *iav-PlexB*^{EcTM} and *iav-TNT* larvae are significantly lower compared to those observed in *iav-GFP* larvae ($p<0.001$, student t-test).

Movie S1, related to Figure 7: Startle response of a single Wild-type *Drosophila* larvae to vibration.

Prior to vibration onset, a single *Drosophila* larva is observed engaging in normal foraging behavior on the dish. It mostly crawls straight and occasionally turns. Vibration (onset of tone) induces stopping, head turning, and a change in larval crawling direction.

Movie S2, related to Figure 7: Analyses of a group of larvae following a vibration stimulus.

This movie, captured by the Multi-Worm Tracker (MWT) software, shows contours and skeletons of larvae before, during, and after the vibration stimulus. Data from only isolated larvae are selected by MWT and subjected to further analyses. Onset of the vibration stimulus (of one second total duration) occurs at 5sec and induces stopping and then head turning, resulting in a significant increase in larval skeleton curvature. The absolute angle between the head (20% of skeleton) and the main body axis (remaining 80% of skeleton) is the measure of the startle reaction to vibration.